Hindawi
Journal of Nanomaterials
Volume 2017, Article ID 1804178, 23 pages
https://doi.org/10.1155/2017/1804178

Review Article

Characterization and Analytical Separation of Fluorescent Carbon Nanodots

Qin Hu,[1] Xiaojuan Gong,[2] Lizhen Liu,[3] and Martin M. F. Choi[1]

[1]*Department of Chemistry, Hong Kong Baptist University, 224 Waterloo Road, Kowloon Tong, Hong Kong*
[2]*Research Center of Environmental Science and Engineering and School of Chemistry and Chemical Engineering, Shanxi University, Taiyuan 030006, China*
[3]*College of Chemistry and Chemical Engineering, Shanxi Datong University, Datong 037009, China*

Correspondence should be addressed to Qin Hu; 11467606@life.hkbu.edu.hk and Martin M. F. Choi; mmfchoi@gmail.com

Received 15 March 2017; Revised 22 May 2017; Accepted 24 May 2017; Published 26 October 2017

Academic Editor: Miguel A. Garcia

Carbon nanodots (C-dots) are recently discovered fluorescent carbon nanoparticles with typical sizes of <10 nm. The C-dots have been reported to have excellent photophysical and chemical characteristics. In recent years, the advances in the development and improvement in C-dots synthesis, characterization, and applications are burgeoning. In this review, we introduce the most commonly used techniques for the characterization of C-dots. The characterization techniques for C-dots are briefly classified, described, and illustrated with applied examples. In addition, the analytical separation methods for C-dots (including electrophoresis, chromatography, density gradient centrifugation, differential centrifugation, solvent extraction, and dialysis) are included and discussed according to their analytical characteristics. The review concludes with an outlook towards the future developments in the characterization and the analytical separation of C-dots. The comprehensive overview of the characterization and the analytical separation techniques will safeguard people to use each technique more wisely.

1. Introduction

During the past few decades, the combination of nanotechnology with numerous disciplines of science have driven the search of new advanced nanoscale materials as a particular interest for scientists [1]. In particular, the functionalized carbon nanodots (C-dots), as an emerging photoluminescent (PL) nanomaterial, have gained considerable attention of the scientific communities owing to their superior structural, photophysical, and chemical properties over other materials. In fact, they have been a multidisciplinary researched nanomaterial in recent years.

The discovery of C-dots stretches back to 2004 when Xu et al. [2] performed gel electrophoretic separation of single-walled carbon nanotubes (SWCNT) synthesized by arc-discharge methods. During the course of their investigation, the suspension was separated into three classes of materials, among which, they observed a fast moving band of nanomaterial that displayed fluorescence under the ultraviolet (UV) light. The fluorescent nanomaterial was further analyzed and fractionated into three components which displayed different fluorescence colors under the UV light. Since this serendipitous discovery, much research efforts have been dedicated to the study of C-dots.

In general, the synthetic methods for C-dots include arc-discharge [2], electrochemical oxidation [3–5], laser ablation [6–9], hydrothermal synthesis [10–15], pyrolysis [16–19], microwave-assisted heating [20–26], plasma treatment [27], neutralization heating [28], and sonication treatment [29] (Scheme 1). All these synthetic methods allow, up to some extent, preparing moderately high-quality C-dots with relatively high PL performance and small size. However, some of these synthetic methods suffer from limitations such as time-consuming treatment process, requirement of strong acids for catalysis, high energy consumption, and complex equipment set-up. Recently, there is a considerable interest in developing labor, material, and energy efficient synthetic methods for C-dots such as carbonization of naturally available bioresources [15, 19, 24, 26, 27, 30–37], preparation with low heating temperature [38], and synthesis without external

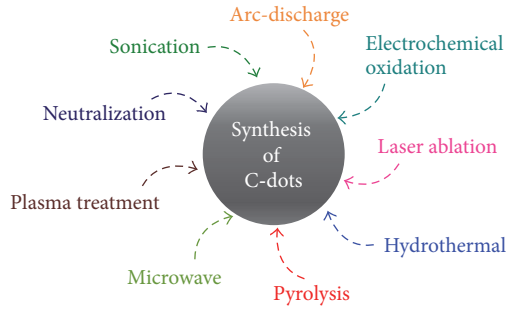

Scheme 1: Schematic illustration of the synthetic methods for C-dots.

heating [39, 40]. In addition, the flexibility in modification and functionalization of the C-dots surface has opened many possibilities in the incorporation of heteroatoms such as nitrogen [15, 20, 21, 37–46], sulfur [33, 46–49], phosphorous [39, 49], and silane [50] into C-dots framework to enhance the PL properties of C-dots.

Many scientists have reported the unique properties of C-dots that exceed those of any previously existed materials. They include diameters below 10 nm with discrete, quasi-spherical, nanocrystalline, or amorphous carbon structures; broad excitation wavelengths (λ_{ex}); tunable fluorescence emission; excellent photostability; high quantum yield (QY); high sensitivity and selectivity targeting specific analytes; favorable biocompatibility; low cytotoxity (a promising nontoxic alternative to heavy-metal-based traditional semiconductor quantum dots); and large Stokes shifts [51–53]. Regarding their surface chemistry, it has been widely described that the C-dots surface is typically attached with many carboxylic acid moieties, which on one hand largely enlarges their potential for further functionalization with small (inorganic/organic) molecules, and on the other hand ideally imparts them with excellent water solubility, facilitating their purification and characterization.

Concerning the applications of C-dots, significant achievements have come up in a variety of scientific fields. Followed by the first report by Cao et al. [54] who demonstrated that C-dots can penetrate easily through cell membrane and are used for conventional bioimaging, a further development occurred at the hands of Yang et al. [55]. Yang et al. succeeded in using C-dots for the in vivo studies of optical imaging with mice for animal test. Followed by these, as a result of extensive and multidisciplinary efforts, C-dots have found their place in a wide range of applications in nanoprobes [56–66], drug delivery [67–71], therapy [72–76], and optoelectronic devices [77–82].

Building upon the great interest in developing novel synthetic methods and searching for new applications for this newly found nanomaterial, one has to fully understand the fundamental properties of C-dots products. Due to the intensive research efforts carried out in the past decades, the scientific community nowadays understands much better the structural, photophysical, and chemical properties of C-dots; however, the complete characterization of C-dots mixture still remains unachieved and faces noteworthy challenge. This is due to the fact that a C-dots product exists as a complex mixture comprising components with various sizes and different surface functionalities, and a polydisperse C-dots sample only represents the summation or average properties of all individual C-dots species [95, 100, 101]. In this sense, there is an urgent need for the development of efficient analytical separation methods to isolate high-purity C-dots fractions for more precious investigation of their unique chemical and photophysical properties. Since the first isolation of C-dots from SWCNT by polyacrylamide gel electrophoresis (PAGE) in 2004 [2], the reports associated with analytical separation techniques of C-dots are emerging. Impressive successes in this area include not only electrophoresis [94, 102–106], but also chromatography [91, 95–97, 100, 101, 107–109], density gradient centrifugation [29], differential centrifugation [98, 110], solvent extraction techniques [99, 111–113], and dialysis [20, 21, 87, 98, 114, 115].

In this current review, without pretending to being exhaustive, we for the first time provide a broad vision of characterization and analytical separation techniques for C-dots by means of 190 references published in 2004–2017, leaving aside the synthesis and applications of C-dots which have been comprehensively reviewed by a set of thorough reviews [52, 116–118]. In addition, some of the merits and drawbacks of the given separation and analytical techniques for C-dots are also highlighted. The main objective of this review is to arouse the interest of the nanoparticles (NP) community in the significance and the importance of characterization and analytical separation of NP so as to truly reveal the NP identity.

2. Characterization Techniques

The chemical composition, size, shape, and structure are important factors that determine the particular and unique properties of C-dots; therefore, numerous efforts have recently been made to explore the reliable and robust characterization tools for C-dots. In this section, as indicated by Scheme 2, all the past and updated characterization techniques for C-dots are discussed in detail.

2.1. Microscopic and Diffraction Techniques. Different nondestructive imaging and microscopic techniques have been developed for the morphology and size characterization of nanoparticles. For the particle size measurement, microscopy is the only method that can directly observe and measure the individual nanoparticles. The microscopic techniques that have been developed for measurements of C-dots include electron microscopic and diffraction techniques such as scanning electron microscopy (SEM), transmission electron microscopy (TEM), atomic force microscopy (AFM), and X-ray diffraction (XRD).

2.1.1. Scanning and Transmission Electron Microscopies. Both SEM and TEM are useful electron microscopy techniques that provide information about the particle size, size distribution, and morphology of C-dots [83, 84, 119–122]. The SEM and TEM images can also be used to investigate whether the agglomeration of particles is present or whether the good

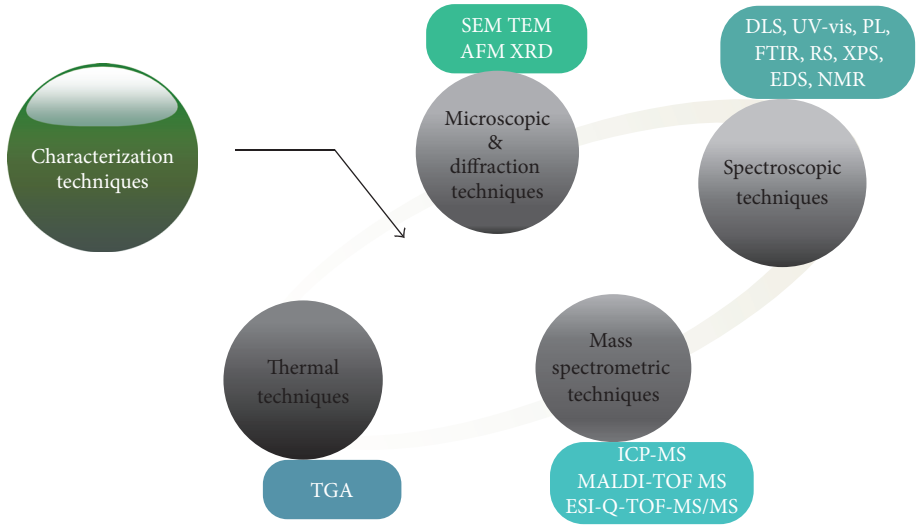

Scheme 2: Schematic illustration of the characterization techniques for C-dots.

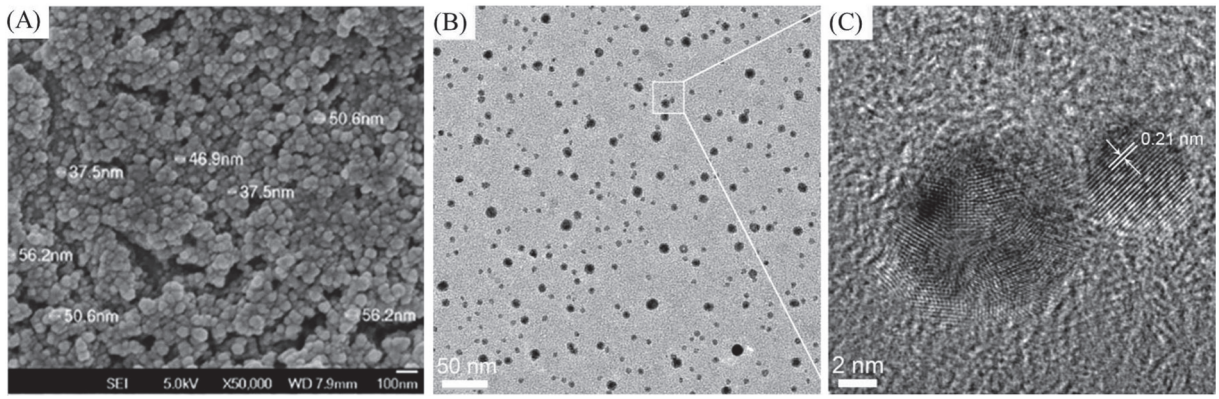

Figure 1: (A) SEM [83], (B) TEM [84], and (C) HRTEM [84] image of a bulk sample of C-dots.

dispersion of particles is achieved. SEM produces images by scanning the surface of a C-dots sample with a focused electron beam which interacts with the atoms of C-dots during which the charges are accumulated to form an image. Figure 1(A) shows an example of SEM image of C-dots [83]. In cases where the measurements exceed the resolution of SEM (1–20 nm), TEM which affords a much higher resolving power (about 0.2 nm) is favored [123, 124]. In TEM, a beam of high-energy electrons is applied to obtain images of the sample based on the electron transmission of C-dots. The average diameter of C-dots can be estimated by randomly counting the particle size on the TEM images. Recently, high-resolution TEM (HRTEM) which uses both the transmitted and the scattered beams to create an interference image has been extensively and successfully used for analyzing C-dots structures and lattice imperfections. Figures 1(B) and 1(C) display an example of TEM and HRTEM image of C-dots [84], which shows that the C-dots have crystalline structure and the lattice spacing distance was about 0.21 nm, which is close to that of the graphite (100) plane.

2.1.2. Scanning Probe Microscopies. AFM is a high-resolution scanning probe microscopy which provides dimensional surface images of C-dots at resolution lower than 1 nm [85, 125–128]. Compared to SEM and TEM techniques, AFM not only produces two-dimensional (2D) images of C-dots from which the C-dots dimension can be determined by randomly counting the height of particles on the images but also provides three-dimensional (3D) information about the surface morphology of C-dots. Figures 2(A) and 2(B) show that both 2D and 3D topographic AFM images of C-dots were achieved through the interaction between the AFM cantilever tip and the C-dots under investigation [85]. Figure 2(C) depicts the height profiles along lines I, II, and III in the 2D AFM image (Figure 2(A)) of C-dots.

Herein, it is important to emphasize that although these microscopy-based techniques are highly accurate and reliable, the electron microscopy requires elaborate sample preparation and acquiring excellent images using these techniques is really challenging. This is because of the fact that this microscopy-based technique has large potential in leading to

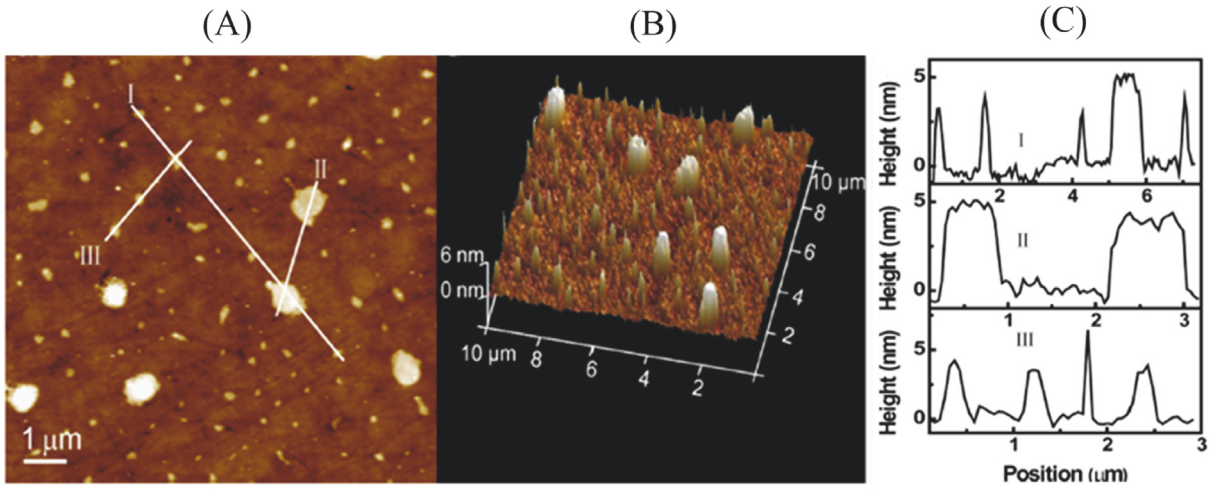

Figure 2: (A) AFM topography image of a bulk sample of C-dots on quartz substrate. (B) AFM 3D image of (A). (C) Height profiles along lines I, II, and III in (A) [85].

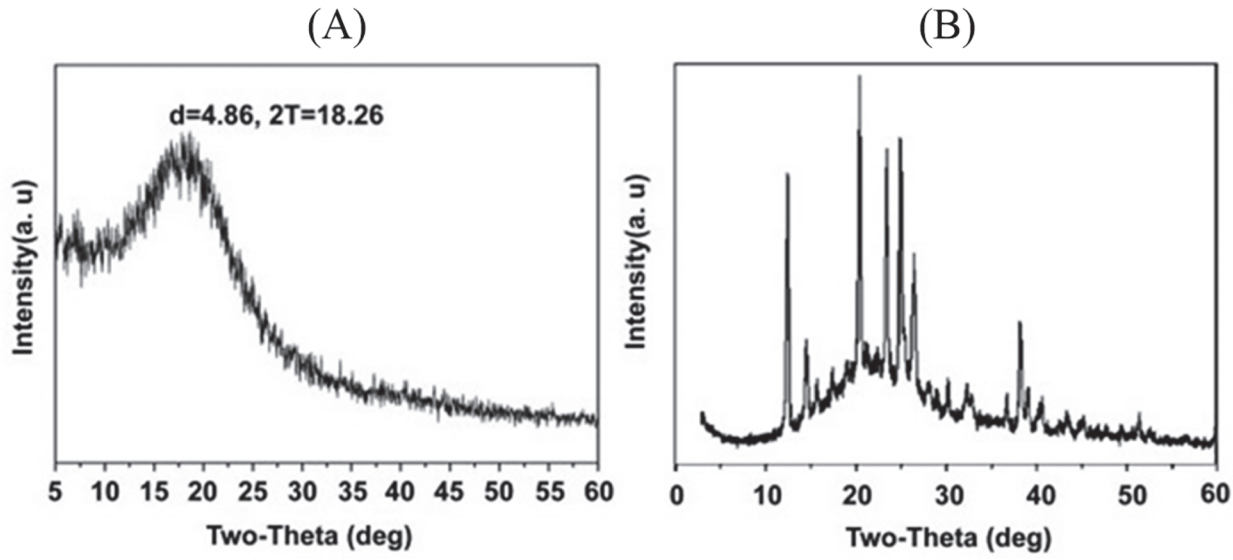

Figure 3: (A) XRD pattern of C-dots-PEI derived from microwave-assisted pyrolysis of glycerol and branched PEI [86]. (B) XRD pattern of C-dots from neutralization heating of glucose [28].

imaging artifacts due to previous sample preparation process (agglomeration of the C-dots sample on the grid) and the vacuum conditions in sample chamber [129].

2.1.3. X-Ray Diffraction. XRD is a rapid analytical technique used for phase identification and characterization of crystalline materials based on their diffraction patterns. When the X-rays interacts with a crystallite C-dots sample, the constructive interference is produced, and these diffracted X-rays are then detected, processed, and counted, revealing the average structure of C-dots [86, 87, 89, 130–136]. Figure 3(A) displays a typical XRD pattern of polyethylenimine (PEI) functionalized C-dots (C-dots-PEI) derived from microwave-assisted pyrolysis of glycerol in the presence of branched PEI [86]. In addition, XRD also provides the information about the purity of an as-synthesized C-dots sample. A recent paper [28] reported that XRD can be applied to estimate the purity of C-dots synthesized from glucose by neutralization heating method. As indicated by Figure 3(B), several impurity peaks were observed in the XRD pattern of C-dots due to the incomplete carbonization of glucose. Although the XRD is a valuable characterization tool for obtaining the critical features of C-dots with a crystallite structure, it is not applicable to characterizing amorphous C-dots.

2.2. Spectroscopic Techniques. Diverse spectroscopic techniques have been described for C-dots characterization, including dynamic light scattering (DLS), ultraviolet-visible (UV-vis), and photoluminescence (PL) spectroscopy,

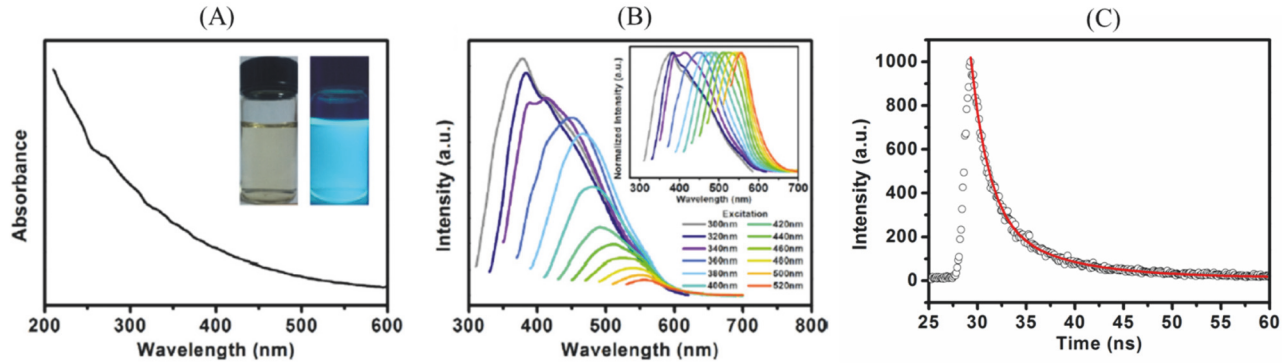

FIGURE 4: (A) UV-vis absorption spectra, (B) PL spectra at different λ_{ex}, and (C) time-resolved PL spectra of S-C-dots derived from waste frying oil. Insets in (A): photographs of the aqueous solution of the C-dots under daylight (left) and UV light (right). Inset in (B): the normalized PL spectra at different λ_{ex} of the S-C-dots [87].

Fourier transform infrared spectroscopy (FTIR), Raman spectroscopy (RS), X-ray photoelectron spectroscopy (XPS), energy dispersive spectroscopy (EDS), and nuclear magnetic resonance (NMR) spectroscopy.

2.2.1. Dynamic Light Scattering. DLS technique has been used to determine hydrodynamic particle size using liquid phase analytical systems equipped with detectors that respond to C-dots in solution. The average C-dots radius can be determined by measuring the diffusion rate of C-dots in liquids. Although there are several typical examples of using DLS for particle size determination of C-dots [24, 69, 120, 127, 136], the application of DLS for the C-dots characterization is not widely utilized. This is due to the fact that the size determination of nanoparticle in a liquid phase using DLS is not reliable since the DLS method provides only a qualitative analysis of the size distribution from the observed photon correlation function [137, 138].

2.2.2. Ultraviolet-Visible and Photoluminescence Spectroscopy. UV-vis and PL spectroscopy are common and widely available spectroscopic techniques that have been used to measure the optical properties of C-dots. Taking together all the information from literatures which characterized C-dots by UV-vis and PL spectroscopy [31, 37, 41, 85, 87, 103, 139], all types of C-dots are active in the UV-vis region of the electromagnetic spectrum, and the fluorescent emission of C-dots shows λ_{ex}-dependent behavior. Recently, the time-resolved PL spectroscopy has been reported to be useful in measuring the photoluminescent lifetime of C-dots [37, 41, 87, 103, 139]. A typical example of UV-vis absorption spectra, PL spectra at different λ_{ex} and time-resolved PL spectra of waste frying oil-derived sulfur-doped carbon dots (S-C-dots) [87], is depicted in Figure 4. In addition, it is important to note that the UV-vis and PL spectroscopy can be used together to determine the QY of C-dots. In detail, the QY of a C-dots sample is determined by a comparative method with quinine sulfate with known QY as the reference. Essentially, the PL spectra of solutions of quinine sulfate and C-dots with identical UV absorbance at the same λ_{ex} are recorded. Hence, a simple ratio of integrated PL intensity of the two solutions will yield the QY of the C-dots [87].

2.2.3. Infrared Spectroscopy. IR is a widely used characterization tool to identify functionalities of the solid materials. In the case of IR analysis of C-dots samples, apart from the evaluation of hydroxyl (-OH) and carbonyl (C=O) functional groups on the C-dots surface [41, 49, 69, 127], IR is also able to examine the doping of heteroatoms into the C-dots framework. Important examples include the identification of the presence of amide/amine (-CN/NH_2) [15, 20, 21, 37–46], alkyl sulfide (C-S) [33, 46–49], organosiloxane (Si-O-Si/Si-O-C) [89, 127, 140, 141], phosphates (P=O and P-O-R) [38, 49, 93], and boronic acid (B-O and B-N) [114, 142, 143] moieties attached on the surface of C-dots, providing evidence for introduction of nitrogen (N), sulfur (S), silicon (Si), phosphorus (P), and boron (B) heteroatoms into C-dots. The merits of this technique for the characterization of surface functionalization of C-dots are being low cost, simple, rapid, and easy for sample preparation. However, the IR cannot give the fine structure information of C-dots, and doping with metal heteroatoms such as aluminum (Al), magnesium (Mg), and nickel (Ni) into C-dots cannot be revealed by IR. Fortunately, other techniques such as XPS provide supplementary information in this aspect, which will be covered in the later part of this review.

2.2.4. Raman Spectroscopy. RS is one of the commonly used nondestructive and noninvasive spectroscopic techniques that have been used for the identification of the state of carbon of a given C-dots sample. Raman spectra of C-dots usually present two main first-order bands [3, 27, 32, 41, 88, 129, 144–149]. The D band represents the vibrations of carbon atoms with dangling bonds in the termination plane of disordered graphite or glassy carbon. The G band (graphitic band) is associated with the vibration of sp^2-bonded carbon atoms in a 2D hexagonal lattice. A common way to estimate the purity (degree of disorder or graphitization) of a C-dots sample is the ratio of the intensities of the disordered D band and crystalline G band (D/G). The C-dots sample with amorphous

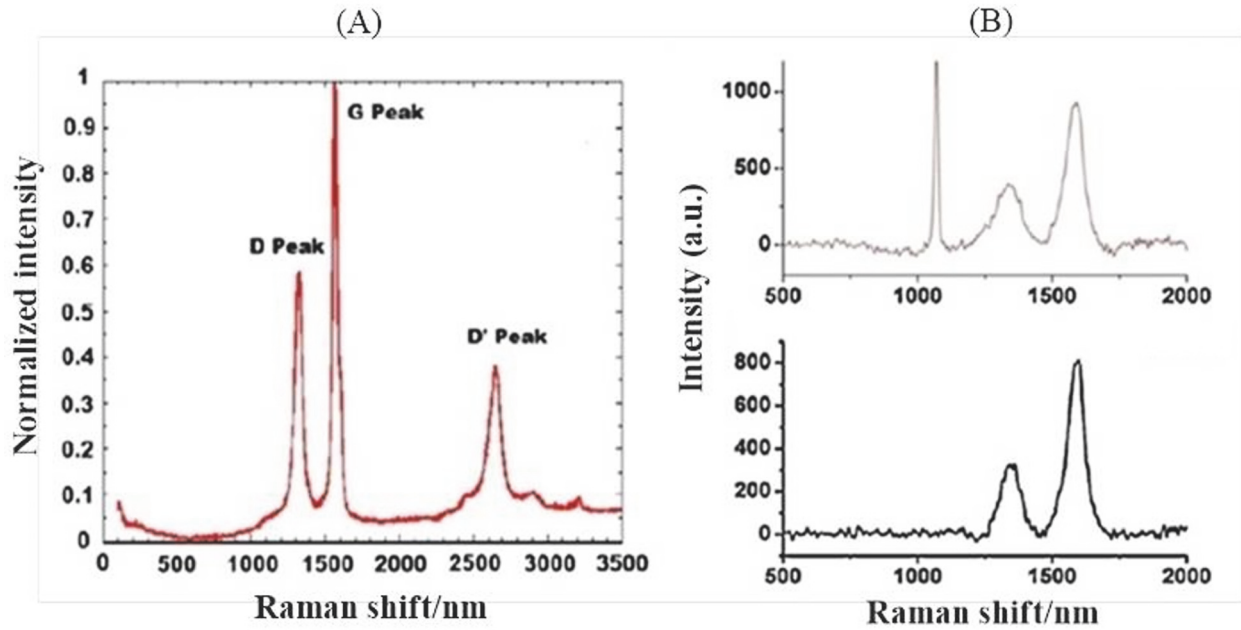

Figure 5: (A) Raman spectrum of C-dots from thermal decomposition of *Trapa bispinosa peel* [32]. (B) Raman spectra of C-dots and F-C-dots [88].

nature has a high D/G ratio. High degree of graphitization of the C-dots sample is indicated by a relatively lower D/G ratio. A typical RS spectrum of C-dots from thermal decomposition of *Trapa bispinosa peel* is shown in Figure 5(A) [32]. In this case, the C-dots had both D (1331 cm^{-1}) and G (1578 cm^{-1}) bands, and the resulting D/G ratio of 0.59 indicates the nanocrystalline graphite structure of C-dots. An additional D′ band located at 2654 cm^{-1} explains the sp^2 hybridization pattern. RS has also been used for size determination of C-dots based on the inverse relationship between the grain size and the D/G ratio. Khanam et al. [88] demonstrated the possibility of using RS technique to determine the grain size of C-dots and C-dots functionalized with hydroxyl and methoxy (F-C-dots) (Figure 5(B)). The relationship between the grain size and the intensity ratio is given by grain size = $44[I_{(D)}/I_{(G)}]$ (in Å). By using this equation, the grain sizes of C-dots and F-C-dots were determined to be 11 nm and 7.3 nm, respectively. Herein, it should be noted that although RS technique is powerful in the characterization of C-dots, several reports stated the difficulty [150] or failures [52, 151, 152] in acquiring a high-quality RS of C-dots sample due to the intense fluorescence of C-dots, resulting in covering the characteristics of the Raman signal.

2.2.5. X-Ray Photoelectron Spectroscopy. XPS is a surface chemical analysis technique that provides information on surface properties, elemental composition, and electronic state of the elements that exist within a material. A XPS spectrum is obtained by irradiating the sample with a beam of X-rays while simultaneously measuring the number of electrons and kinetic energy. For the characterization of C-dots, XPS has generally been used for the assessment of the elemental composition and the chemical bonds of C-dots in combination with IR. Doping of C-dots with nonmetallic heteroatoms such as N [43, 49, 56, 99, 114, 121, 122, 134], S [14, 24, 46, 49, 87], Si [50, 127, 140, 141], P [39, 49, 93], and B [114, 142] has been characterized by XPS. A typical example of XPS analysis employed to estimate the surface states and chemical composition of nitrogen and sulfur-codoped C-dots (SNCNs) was displayed in Figure 6 [46]. In addition, the incorporation of C-dots with metal heteroatoms such as Al [153], Mg [154], and Ni [155] that cannot be detected by IR has also been demonstrated by XPS. Although XPS is very valuable in the characterization of elemental composition and functionalities of C-dots, it does not generally have the spatial resolution to examine individual nanoparticles.

2.2.6. Energy Dispersive Spectroscopy. EDS, which is also called energy dispersive X-ray analysis, is another commonly used technique for the elemental analysis of a sample. In EDS, a high-energy beam of X-rays is focused onto the sample to be analyzed, and an X-ray spectrum is obtained by measuring the number and energy of the X-rays emitted from a specimen with an energy dispersive spectrometer. In general, all of the chemical elements are active in EDS [from beryllium ($z = 4$) to uranium ($z = 92$)], and qualitative (from the peak energy) and quantitative (from the peak intensity) analyses can be carried out on the basis of the lines present in the simple X-ray spectra [156]. The main application of EDS for C-dots characterization is to analyze the elemental composition of C-dots, for example, the contents of carbon (C), oxygen (O), and other doped elements such as Si [89, 137, 139]. In addition, EDS is able to provide information about the purity of C-dots [32, 157, 158]. Figure 7 displays an

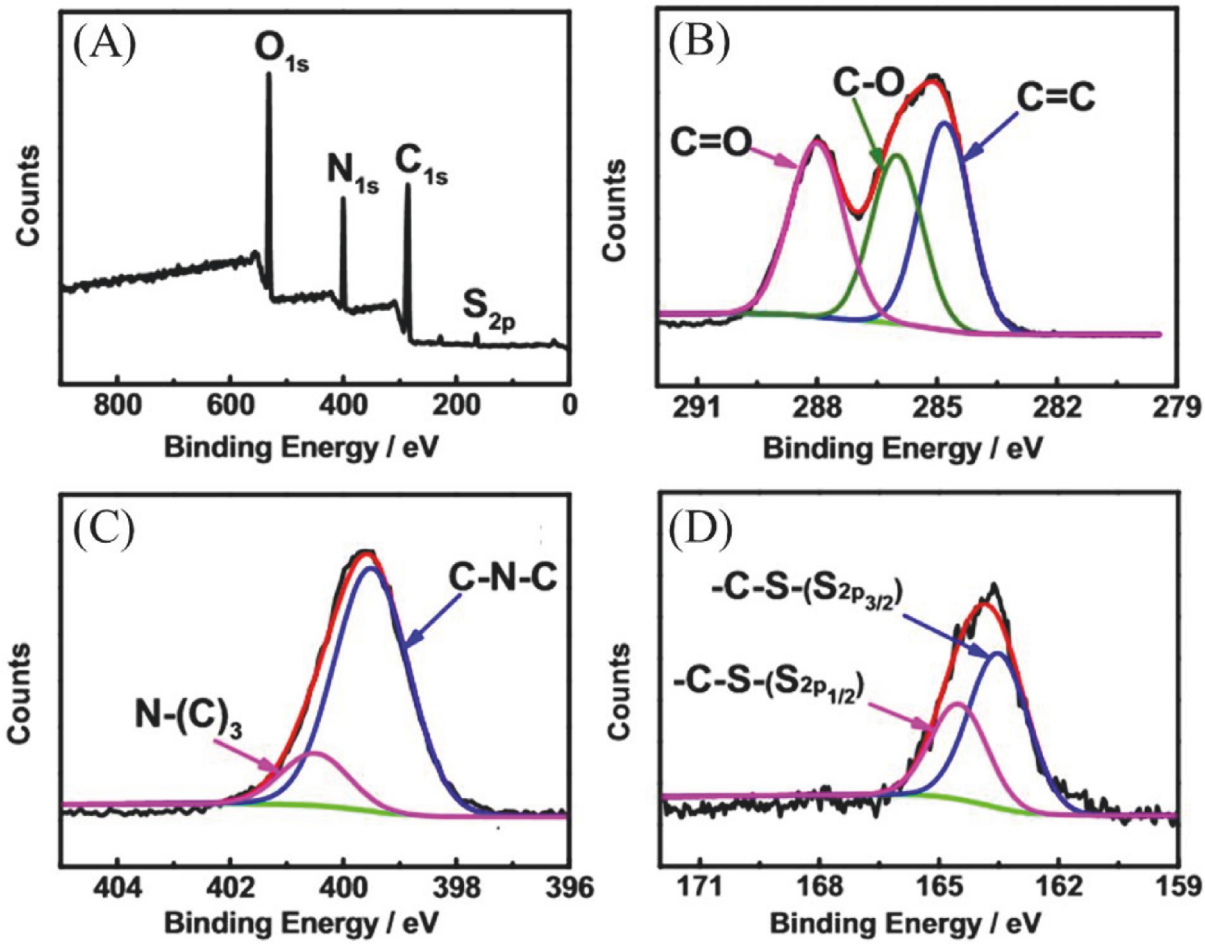

Figure 6: Survey (A) and high-resolution C_{1s} (B), N_{1s} (C), and S_{2p} (D) XPS spectra of SNCNs [46].

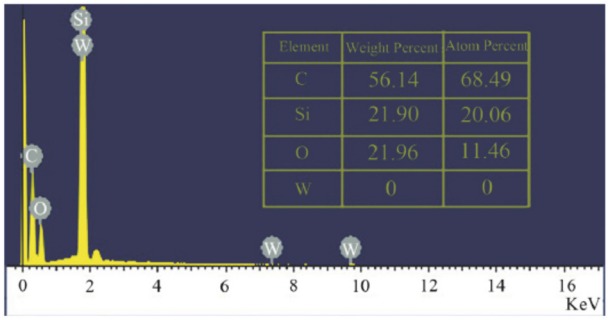

Figure 7: The EDS data of C-dots passivated with AEAPMS [89].

EDS spectra of C-dots passivated with *N*-(*β*-aminoethyl)-*γ*-aminopropyl methyldimethoxy silane (AEAPMS) [89]. Apart from obtaining the C, O, and Si contents, small impurity peaks of tungsten (W) were found to be coexisting in the as-synthesized C-dots sample.

2.2.7. Nuclear Magnetic Resonance Spectroscopy. NMR spectroscopic technique has also been used to gain further

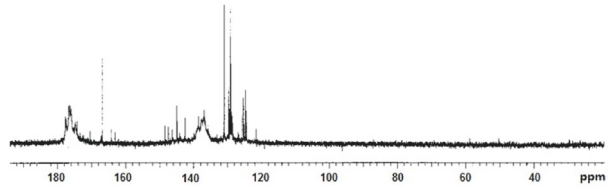

Figure 8: ^{13}CNMR spectrum of C-dots in D_2O, showing the presence of sp^2 carbon atoms [90].

structural insights into C-dots. The main application of NMR for the characterization of C-dots aims to precisely identify the surface functionality of C-dots, to determine the element states (e.g., C, N, and P) in C-dots, and to examine the nature of their bonding onto the particle surface. Tian et al. [90] firstly reported the utility of ^{13}CNMR spectroscopy in liquid state to identify the carbon states in a C-dots sample derived from candle shoot (Figure 8). Followed by this, numerous efforts have been contributed to using NMR spectroscopy in both solid state and liquid state for C-dots characterization [21, 38, 56, 85, 109, 115, 135, 143, 159–164]. In addition, NMR has been proved to be powerful in the establishment of the

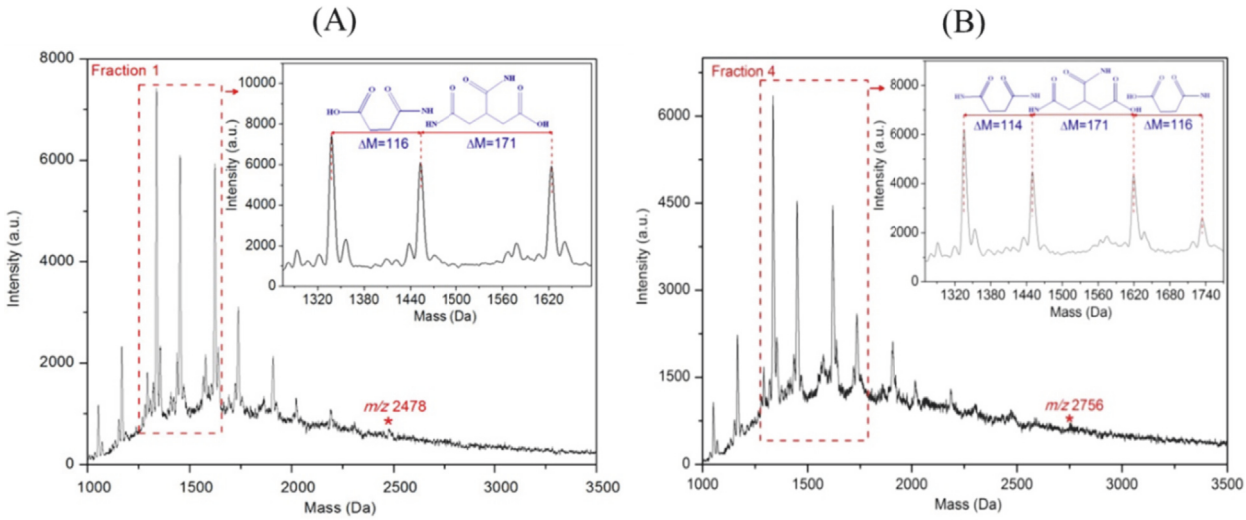

Figure 9: Representative MS spectra from MALDI-TOF MS analysis of fractions 1 and 4, respectively [91].

chemical alterations that happened to the surface modifiers during carbonization. For instance, Khanam et al. [88] applied ^{1}H NMR characterization to follow the conversion of methoxy group to hydroxyl group on the surface of F-C-dots during the reaction process, and Nandi et al. [165] applied ^{1}HNMR to confirm the transformation of the glucose residues into elemental carbon and the presence of coating alkyl chains. Although the NMR technique has merits in nondestructive nature and easy sample preparation, it is very expensive, time-consuming, and less sensitive in comparison to mass spectrometric techniques.

2.3. Mass Spectrometric Techniques. Mass spectrometry (MS) has been reported to be powerfully useful in elucidating the chemical structures of smaller-sized nanoparticles (<5 nm) [166]. The mass spectrometric techniques that have been applied to characterize C-dots include inductively coupled plasma-mass spectrometry (ICP-MS), matrix-assisted laser desorption/ionization time-of-flight mass spectrometry (MALDI-TOF MS), and electrospray ionization quadrupole time-of-flight tandem mass spectrometry (ESI-Q-TOF-MS/MS).

2.3.1. Inductively Coupled Plasma-Mass Spectrometry. ICP-MS is a type of mass spectrometry that has been widely used for determination and quantification of inorganic nanoparticles such as gold and nickel particles [167–169]. However, ICP-MS is not widely used for the measurement of inorganic nanoparticles. For the ICP-MS measurement of C-dots, only Bourlinos et al. [114] reported the use of ICP-MS for the characterization of B-doped C-dots so far. In their study, the exact amount of the B-doped C-dots sample was determined by ICP-MS using boronic acid as the calibration standard. The content of B (3%) was in accordance with the result obtained by XPS.

2.3.2. Matrix-Assisted Laser Desorption/Ionization Time-of-Flight Mass Spectrometry. MALDI is a soft ionization technique that has been widely used for the structural characterization of NP [170–172]. TOF analysis is based on accelerating a set of ions to a detector where all of the ions are given the same amount of energy, and the determination of the mass of ions is according to their different flight times. MALDI-TOF MS analysis gives mass accuracy better than 0.1. Based on this aspect, it has recently been used to characterize C-dots. Khanam et al. [88] for the first time applied MALDI-TOF MS to acquire the molecular weight of rare C-dots and F-C-dots. The determination was carried out by using three different matrix materials, namely, sinapinic acid (SA), 2,5-dihydroxy benzoic acid (DHBA), and α-cyano-4 hydroxycinnamic acid (HCCA) (Figure 9). The molecular weight obtained with these matrices was the same and the molecular weights for C-dots and F-C-dots were 267 m/z and 392 m/z, respectively. Soon afterward, our group reported the utility of MALDI-TOF MS for the characterization of the surface-attached functionalities on C-dots by examining their fragmentation patterns [91, 96, 108]. One typical example is the structural elucidation of C-dots obtained by microwave-assisted pyrolysis of citric acid and 1,2-ethylenediamine [91] (Figure 9). The C-dots mixture was firstly separated by RP-HPLC, after which, the fractions were collected and further characterized by MALDI-TOF MS in positive ionization mode under a pulsed N_2 laser (337 nm). We demonstrated that each of the C-dots fractions shows their unique fragmentation pattern, closely relating to their surface-attached carboxylic acid and amide/amine moieties. The MALDI-TOF MS technique is powerful in identifying the functionalities of C-dots; however, this technique exhibits lower sensitivity with increasing mass and is not capable of capturing the larger ions in high mass range.

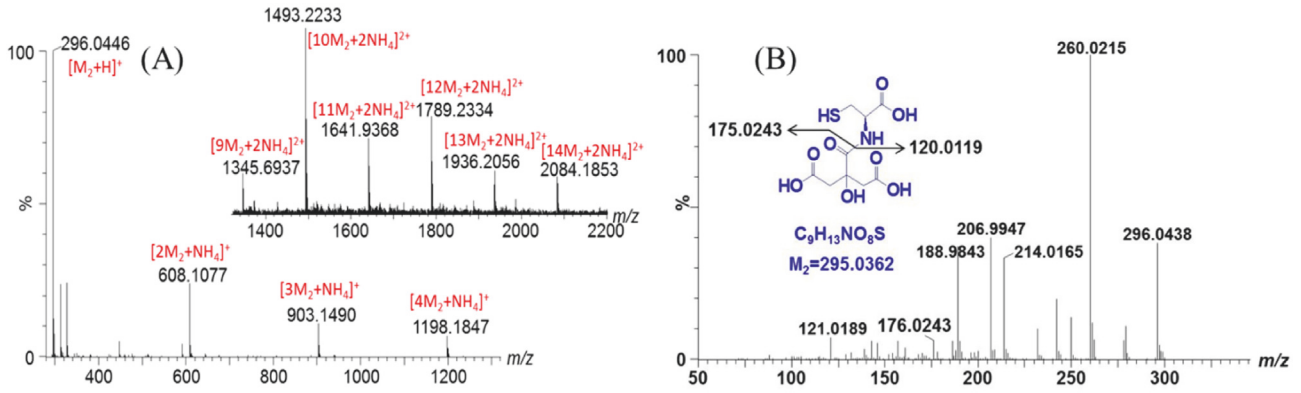

Figure 10: Representative (A) MS and (B) MS/MS spectra from ESI-MS analysis of fraction 2. Shown in the insets are the MS spectra of the same fraction in the higher m/z ranges [92].

2.3.3. Electrospray Ionization Quadrupole Time-of-Flight Tandem Mass Spectrometry. The electrospray ionization quadrupole time-of-flight tandem mass spectrometry (ESI-Q-TOF-MS/MS) combines the use of soft ionization technique and sensitive MS detection. Till now, our group is the only one that successfully applied ESI-Q-TOF-MS/MS to characterize the chemical composition of C-dots [92, 173]. By coupling the ultraperformance liquid chromatography (UPLC) with ESI-Q-TOF-MS/MS detection, the MS and MS/MS spectra of each separated C-dots fraction were simultaneously captured (Figure 10). Based on high-accuracy MS and MS/MS analyses, we elucidated the chemical structures and obtained the molecular formulas of each C-dots species simultaneously. In particular, our study revealed for the first time that the C-dots species exist as supramolecular clusters with their individual monomers units linked together through noncovalent bonding forces.

2.4. Thermal Techniques. Thermogravimetric analysis (TGA) is the only thermal technique that has been applied to characterize C-dots [27, 32, 56, 69, 88, 93, 158, 174, 175]. In TGA measurement, the instrument continuously weighs a C-dots sample by coupling with FTIR or MS for gas analysis. A weight loss curve was plotted by measuring the amount and the change rate of the weight loss of a C-dots sample with respect to temperature, providing information about the thermal stability of C-dots. For example, Bandosz et al. [93] reported TGA/MS for the characterization of surface functionality of three kinds of C-dots samples. They acquired the TGA curves under the condition that the C-dots samples were heated up to 1000°C (10°C/min) under a constant helium flow (100 mL/min) (Figure 11). The C-dots derived from poly(4-ammonium styrene-sulfonic acid) were determined to have the richest surface groups, especially those decomposing as SO_2 (m/z 64), CO_2 (m/z 44), and CO (m/z 28). Another interesting case is the employment of thermal analysis coupled with FTIR (TGA/FTIR) to record the formation of C-dots from plasma treatment of egg-white [27]. The TGA method has advantages in fast load and low sample amount; however, it only provides meaningful data to certain types of C-dots which show changes in mass during measurements.

3. Analytical Separation Techniques

As mentioned previously, from the viewpoint of better understanding the fundamental properties of C-dots, numerous analytical techniques have been developed for the separation of C-dots obtained from various starting materials. A summary of the separation techniques described in this section is presented in Scheme 3.

3.1. Electrophoretic Techniques. Electrophoretic methods are valuable tools for the separation of water-soluble NP including iron oxide particles [176–178], silver, and gold [179, 180] as well as silicon NP [181] based on particle size, shape, and ionization of the surface functionality of NP. For the electrophoretic separations of water-soluble C-dots, gel electrophoresis (GE) [2, 102, 103] and capillary zone electrophoresis (CZE) [94, 104–106] have been reported.

3.1.1. Gel Electrophoresis. GE is a fractionation technique which allows the analytes to be separated according to the different migration behavior of analytes by sieve effects under the influence of an electric field. Xu et al. [2] firstly reported the separation of C-dots by PAGE when they were purifying SWCNT derived from arc-discharge soot. The oxidized candle-soot mixture was separated in a 20% denaturing gel (8 M urea, 1x TBE running buffer) by applying 600 V at 55°C in an electrophoresis unit. As indicated by Figure 12(A), when observed under UV light, the candle-soot dispersion was separated into three classes of nanomaterial, that is, agglomerates which did not penetrate the gel, slow moving dark bands of short tubular carbons, and fast moving multicolor bands of fluorescent nanomaterials. The multicolor fluorescent bands were further separated into three discrete bands, displaying different colors in order of their elution and increasing size (Figure 12(B)). After separation, the isolated C-dots fractions were passed through a 0.45 μm PVDF filter and extensively dialyzed against distilled water for purification and subjected to further characterization by elemental analysis, FTIR, PL

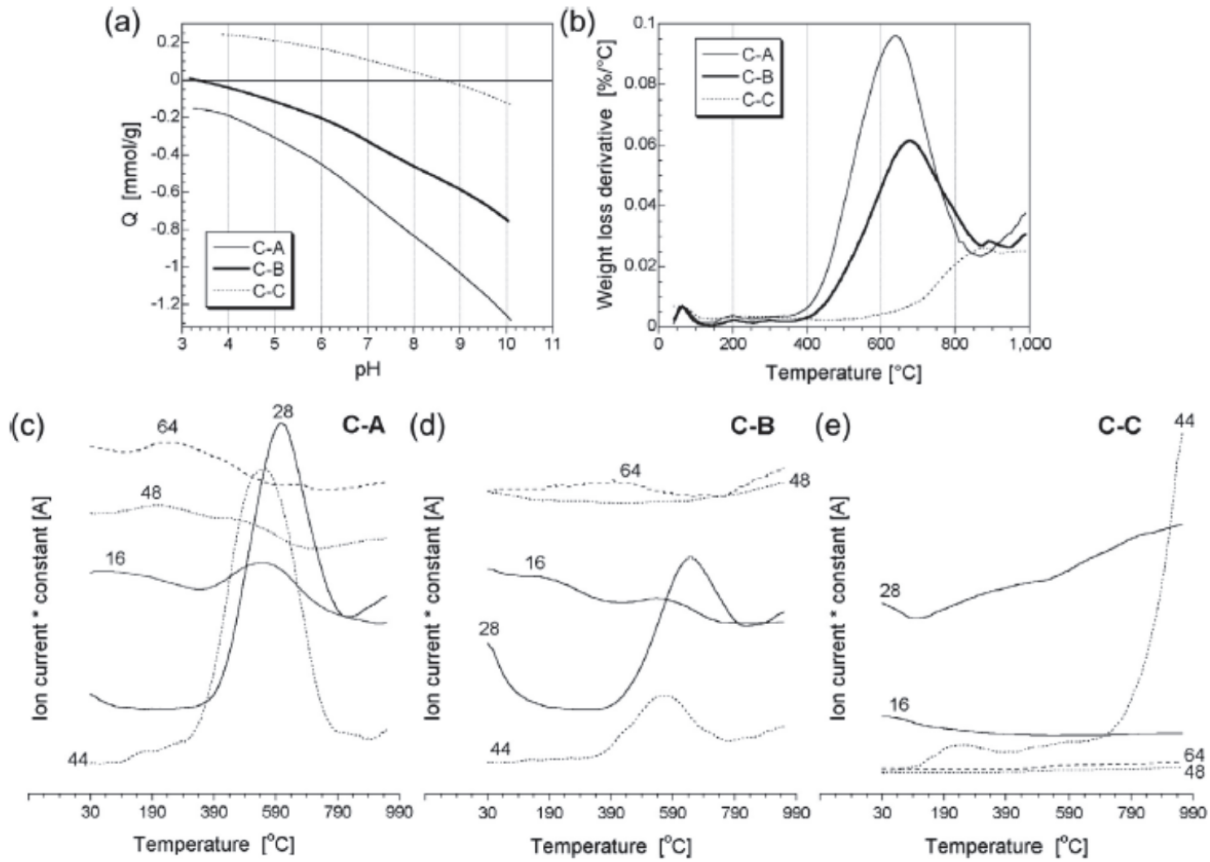

FIGURE 11: Characterization of the surface chemistry of three kinds of C-dots derived from different materials: (a) proton binding curves of C-dots samples. (b) DTG curves of C-dots samples in helium. ((c)–(e)) Selected MS patterns of C-dots samples (multiplication factor: MW-16 ([O]) × 7; MW-28 (CO) × 1; MW-44 (CO_2) × 5; MW-48 (SO) × 500; MW-64 (SO_2) × 500) [93].

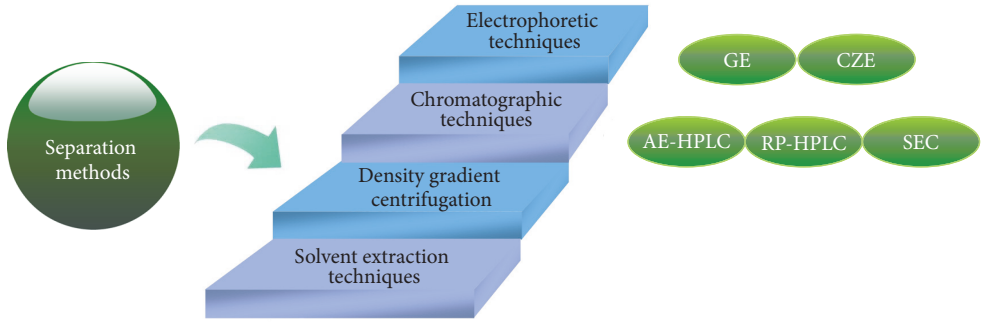

SCHEME 3: Schematic illustration of the separation techniques for C-dots.

spectroscopy, and AFM. Afterwards, Liu et al. [51] reported the sodium dodecyl sulfate- (SDS-) PAGE method for the separation of C-dots sample. Similar to the observations of Xu et al. [2], the electrophoretic mobilities of C-dots fractions were highly related to their fluorescence color, with the faster migrating C-dots species emitted at shorter wavelengths. Later, Li et al. [102] used the SDS-PAGE method to explore the interaction between C-dots and tyrosinase (TYR) in the C-dots/TYR hybrid catalysts. The mixture of C-dots and C-dots/TYR hybrids was loaded onto SDS polyacrylamide gels (20%) and electrophoresed at 50 mA. Gel images obtained under the visible light and UV illumination demonstrated that C-dots were connected to the TYR by noncovalent bonds and formed stable complexes. Sachdev et al. [103] also applied SDS-PAGE method for the investigation of multi-color fluorescence of C-dots passivated by polyethylene glycol (PEG) and polyethyleneimine (PEI). The C-dots samples were separated in 12% denaturing gel under an electric field of 120 V. After electrophoresis, the fluorescent bands were excised and visualized under different excitation filters. The

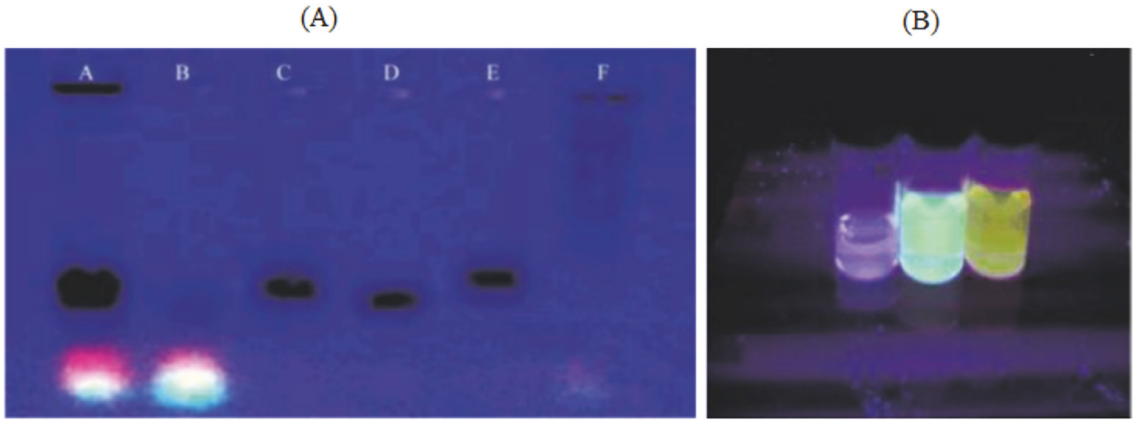

FIGURE 12: (A) Electrophoretic profile of C-dots in 1% agarose gel under 365 nm UV light. (Wells A–C are crude SWNT suspension, fluorescent carbon, and short tubular carbon, resp. Wells D and E are the further separation of fraction C. Well F is the cut SWNT). (B) Photographic images of the 3 fractions of fluorescent C-dots species under 365 nm [2].

excised C-dots-PEI band displayed multicolor fluorescence whereas no fluorescence was observed from excised piece of gel in the C-dots-PEG lane. In addition, they also employed agarose gel electrophoresis (AGE) to study the surface charge-dependent mobility of C-dots. The C-dots samples were loaded in 1.2% agarose gel and run in Tris acetate-EDTA buffer under 85 V. When the gel was visualized using a UV transilluminator, the fluorescent bands of positively charged C-dots-PEI and negatively charged C-dots-PEG migrated towards negative and positive terminals, respectively. In these cases, despite the fact that PAGE has virtue in identifying the relationship between the mobility and color of the fluorescent C-dots, it does not have high separation efficiency since the pore size of the polyacrylamide gel is typically ~3–5 nm [182], which limits its application in separation of C-dots with a wide range of size.

3.1.2. Capillary Zone Electrophoresis. CZE, with remarkable separation efficiency, has rapidly emerged as a useful separation approach for NP [94, 104–106, 183, 184] according to their different electrophoretic mobilities (on the basis of their charge/size ratio) through an electrolyte solution contained in a fused silica capillary under the influence of an electric field. The utility of CZE in conjunction with a diode array detector (230 nm) was firstly reported by Baker and Colón [104] for the separation of C-dots obtained from the flame of an oil lamp. In this study, they comprehensively examined the influence of buffer composition on the electrophoretic pattern of the mixture of negatively charged C-dots by varying buffer type, pH, and concentration. Although CE is a powerful technique that is simple to perform and achieves satisfactory separation efficiency, the benefits provided by the high number of theoretical plates obtained with CE for C-dots separation are overshadowed by its low sensitivity of the UV detection systems owning to the small injection volumes of sample [185]. To overcome the limitation of the low sensitivity and ensure the accuracy for C-dots analysis, our research group separated C-dots by use of commercial CZE apparatus coupled with a diode array detector

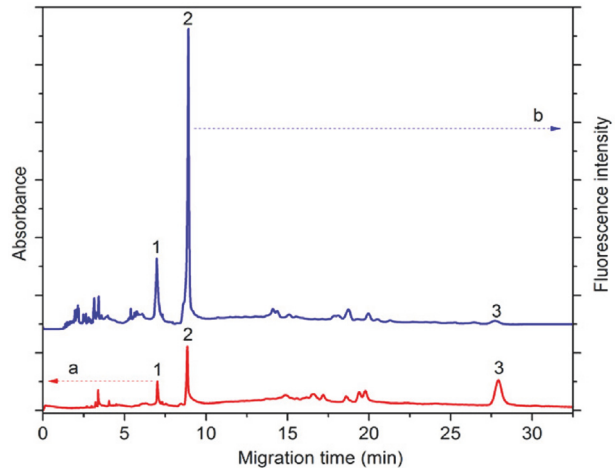

FIGURE 13: Capillary electrophoretic separation of C-dots monitored at (a) absorption wavelength of 250 nm and (b) laser-induced fluorescence at $\lambda_{ex}/\lambda_{em}$ of 488/550 nm. Peaks (1), (2), and (3) are positively charged, neutral, and negatively charged C-dots, respectively [94].

and a laser-induced fluorescence (LIF) detector [94]. The absorption electropherograms of C-dots were acquired at 250 nm and the fluorescence was monitored at excitation wavelengths/emission wavelength ($\lambda_{ex}/\lambda_{em}$) of 488/550 nm. The separation was achieved using 40.0 cm capillary (50 μm i.d. and 325 μm o.d.) with 30 mM sodium acetate-acetic acid (NaAc-HAc) at pH 3.6 as run buffer and an applied voltage of 15 kV. Figure 13 depicts that the combination of UV (curve (a)) and LIF (curve (b)) detection reveals corroborating as well as additional information of the complex C-dots mixture. For example, the electrophoretic behaviors of the positively charged, neutral, and negatively charged C-dots obtained with two detection methods are the same. Peaks (1) and (2) display strong UV and fluorescence signals while peak (3) shows strong absorption but weak emission signals.

This CE method was successfully used to study the reaction time-associated kinetics of C-dots formation and identify the functional groups-associated charge states. Afterwards, our group applied CE coupled with UV detection (250 nm) and LIF detection ($\lambda_{ex}/\lambda_{em}$ 488/550 nm) for the separation of hollow C-dots synthesized from glacial acetic acid and diphosphorus pentoxide without external heating [106]. The separation was achieved using 40.0 cm capillary (50 μm i.d. and 325 μm o.d.) with 10 mM SDS and 30 mM phosphate (pH 9.0) as run buffer at an applied voltage of 15 kV. The separated fractions were also collected and further analyzed by UV-vis and PL spectroscopy, MALDI-TOF MS, and TEM. We can see that CZE is certainly useful in identifying the different charge states of C-dots species present in a complex C-dots mixture. However, due to the low sample injection volume of CZE, the collection of enough amounts of individual CE-fractionated C-dots fractions is extremely time-consuming. Besides, CE can only separate the charged C-dots species rather than neutral C-dots species which eluted out as one single intense peak.

Isoelectric focusing (IEF) is commonly used for the determination of the isoelectric point of macromolecules and bioparticles. The colloidal NP of different sizes can be size-selectively separated from their mixtures in a home-made miniscale IEF unit [186]. This method is rapid, highly sensitive, and inexpensive. However, so far, there is no report on the separation of C-dots using IEF.

3.2. Chromatographic Techniques. The chromatographic techniques, previously proven to be highly efficient in the separation of metal-based quantum dots [92, 172, 173] based on their sizes and chemical properties, have recently been applied to separate and analyze C-dots. Currently, chromatographic methods available for the separation of C-dots are anion-exchange high performance liquid chromatography (AE-HPLC) [95, 100, 101, 107], reversed-phase- (RP-) HPLC [91, 96, 108], and size exclusion chromatography (SEC) [97, 109].

3.2.1. Anion-Exchange High Performance Liquid Chromatography. AE-HPLC is a separation technique which allows the separation of negatively charged ions or molecules according to their affinity to the ion exchange resin containing positively charged groups. Vinci and Colon [95] firstly used AE-HPLC in conjunction with UV detection at 250 nm and laser-induced photoluminescence detection (LIP) at $\lambda_{ex}/\lambda_{em}$ of 325/350 nm to separate C-dots products obtained starting with the soot generated during combustion of paraffin oil in a flame. Solutions of C-dots mixture was fractionated using a strong anion-exchange column and ammonium acetate (NH_4Ac) as eluent (Figure 14(A)). The fractions of C-dots were collected for further characterization by PL spectroscopy (Figure 14(B)) and TEM (Figure 14(C)). The C-dots were demonstrated to be comprised of C-dots species with different optical and electronic properties. Later, the same group employed the previously well-established AE-HPLC method for the high-resolution separation of another kind of C-dots derived from the oxidation of graphite nanofibers [100, 101]. Apart from TEM and spectroscopic studies [100], the authors examined the surface composition of the C-dots fractions that exhibit stronger PL by means of XPS and FTIR [101] and identified that the luminescent NP with the higher luminescence possesses less oxygen content. Similarly, Liu et al. [107] applied AE-HPLC with UV detection at 250 nm to fractionate C-dots capped with PEI. Four fractions were collected, characterized by TEM and FTIR, and finally used for separation and preconcentration of Cr(VI). The C-dots species in smaller size behavior served as promising adsorbents for the separation and preconcentration of Cr(VI) and worked more efficiently as signal-enhancing agents for flame atomic absorption spectrometric determination of Cr(VI) in real water samples.

3.2.2. Reversed-Phase High Performance Liquid Chromatography. RP-HPLC is a separation technique with the polarity of mobile phase higher than that of stationary phase. Compared to CZE, in addition to the preparative scale property of HPLC which allows for the collection of individual fractions of C-dots for more precious study, HPLC using a C18 column can efficiently retain and separate the neutral C-dots species which migrate as one single peak in CZE. Our group [96] firstly proposed the RP-HPLC method for high-resolution separation of C-dots prepared by hydrothermal carbonization of chitosan with UV detection at 300 nm and fluorescence detection at $\lambda_{ex}/\lambda_{em}$ of 300/405 nm. The separation was achieved by using C18 column with methanol (MeOH) and Milli-Q water as the mobile phase (Figure 15(A)). In both cases, the electronic and optical properties of C-dots were measured by UV-vis and PL spectroscopy (inset of Figure 15(A)) and TEM (Figure 15(B)). Similar to the observations of Vinci et al. [95, 100, 101], the as-synthesized C-dots samples were demonstrated to be comprised of numerous C-dots species, displaying their unique optical and electronic properties. Additionally, of particular importance, the MALDI-TOF-MS was applied to elucidate the surface-attached functionalities of C-dots fractions by examining their fragmentation patterns (Figure 15(C)). Later, we adopted RP-HPLC coupled with fluorescence detection (340/440 nm) for the fractionation of C-dots prepared from citric acid and 1,2-ethylenediamine using 10 mM NH_4Ac (pH 4.5) and MeOH as the mobile phase [91]. Our group further reported the separation of hollow C-dots by the above established RP-HPLC method using UV detection (300 nm) with a binary solvent mixture of MeOH and 10 mM NH_4Ac buffer (pH 5.5) as the mobile phase [108]. The fractions collected were found to be multicolor emissive, displaying red, green, and blue fluorescence under UV irradiation (365 nm). Selected fractions with strong PL were proved to be in low cytotoxicity by MTT assay and, therefore, finally used for living cell imaging. Recently, we employed RP-UPLC coupled with either UV detection [187] or MS [92, 173] detection for the separation and analyses of different types of C-dots. A typical example is the utilization of ultraperformance liquid chromatography (UPLC) coupled with ESI-Q-TOF-MS/MS to separate and characterize C-dots derived from microwave-assisted pyrolysis of citric acid and 1,2-ethylenediamine [173]. By using UPLC, the C-dots product was well separated

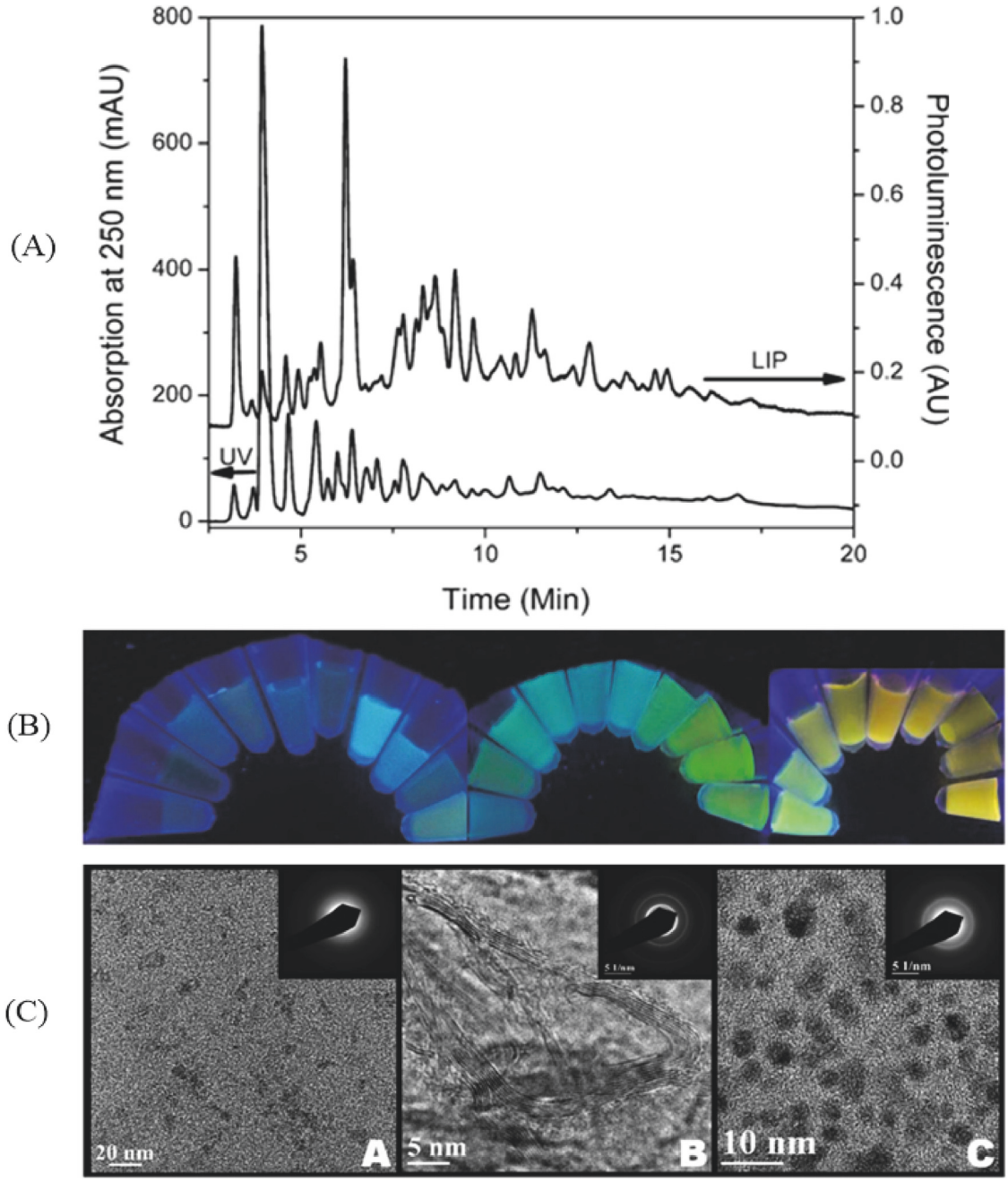

Figure 14: (A) AE-HPLC chromatograms of the soot-derived C-dots sample monitored by UV detection at 250 nm and LIP detection at $\lambda_{ex}/\lambda_{em}$ of 325/350 nm. (B) Photographic images of the 29 separated C-dots fractions under a hand-held UV lamp. (C) TEM images and electron diffraction patterns of selective C-dots fractions (images A–C are attributed to fractions 3, 9, and 28, resp.) [95].

into ten fractions within 4.0 min. By using ESI-Q-TOF-MS/MS, the characterization of the chemical structures and the elucidation of the molecular formulas of C-dots species were achieved simultaneously.

3.2.3. Size Exclusion Chromatography. SEC, also known as gel filtration chromatography, is a size-based separation process with a column with flow channels formed by packing with porous materials. The separation of particles is achieved by their differences in flow velocity. The particles with smaller or equal size of pore in packing materials permeate deeply into the column while larger particles that diffuse freely through it are excluded, resulting in longer retention time for the smaller particles. Recently, SEC has also been used for the separation of C-dots based on their size differences. For example, Wang et al. [109] simply fractionated C-dots passivated with PEG1500N by an aqueous gel column packed with commercially supplied Sephadex G-100 gel with water

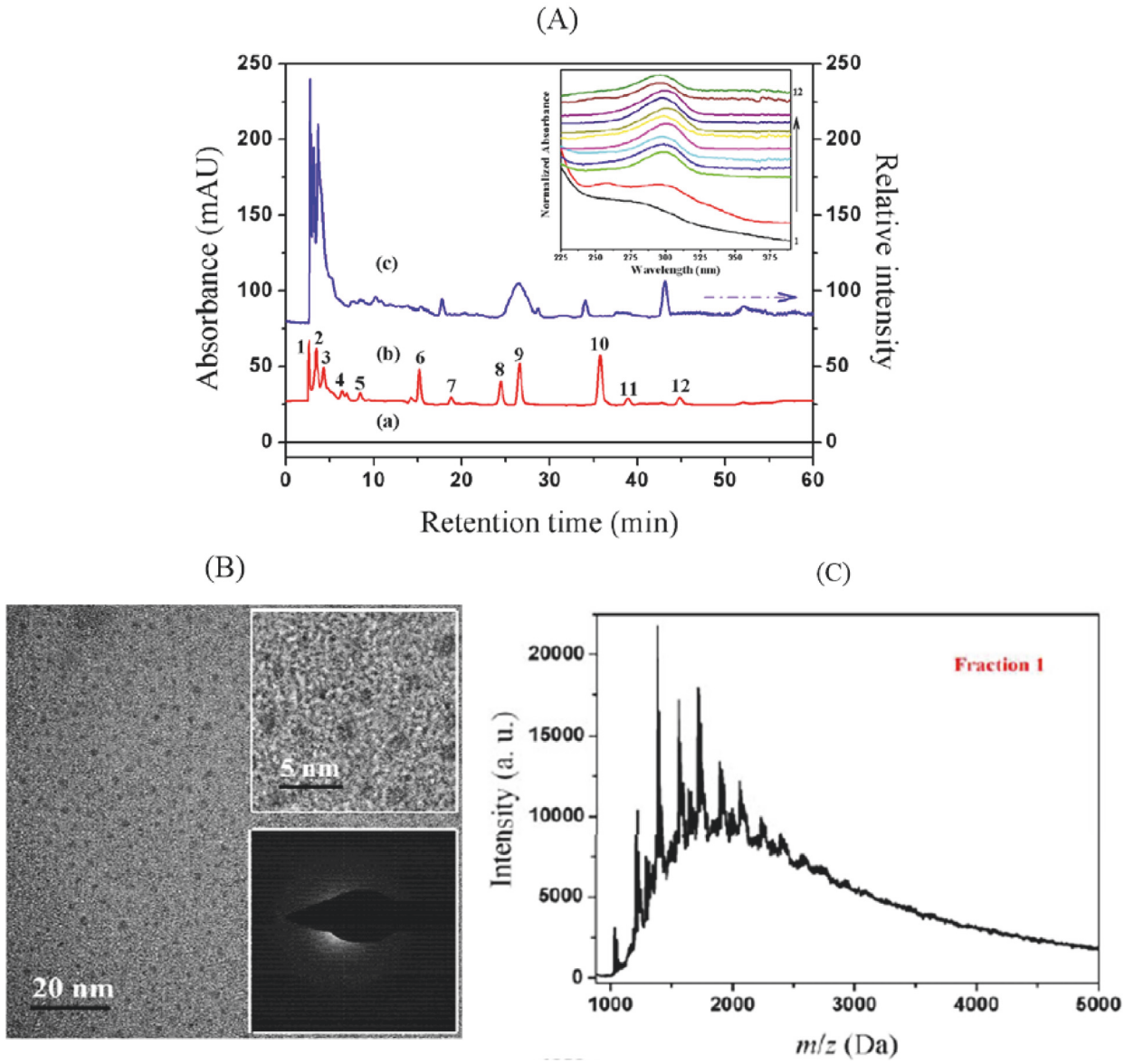

Figure 15: (A) Absorption chromatograms of (a) chitosan and acetic acid in MeOH/water (1 : 19 v/v) and (b) C-dots solution monitored at 300 nm. (c) Fluorescence chromatogram of C-dots solution monitored at $\lambda_{ex}/\lambda_{em}$ of 300/405 nm. The inset displays the absorption spectra of the 12 separated C-dots fractions. (B) and (C) are the TEM image and MALDI-TOF MS spectrum of fraction 1, respectively [96].

as the eluent. The fractions were collected and further characterized by TEM, AFM, ^{13}CNMR, and FTIR analysis. Jiang et al. [97] isolated fluorescent C-dots products from Nescafe® Original instant coffee powder by Sephadex G-25 SEC (Figure 16). In this interesting case, the coffee powder was dissolved in distilled water at 90°C, vigorously stirred to mix, and centrifuged at 14,000 rpm for 15 min. The resulting supernatant was filtered through a 0.22 μm-membrane to remove the large or agglomerated particles and then loaded onto the gel column with distilled water as eluent. The fluorescent C-dots fractions were collected and applied for cell imaging. As indicated by Figure 16, the obtained C-dots fractions display multiple colors when excited at different λ_{ex}.

3.3. Density Gradient Centrifugation. The density gradient centrifugation method which is a routine technique used to separate biomacromolecules also exhibits great potential in isolating NP [188]. Briefly, samples are added on the top of a density gradient formed by sequentially layering solutions of different densities. Upon centrifugation, the particles deposit in the density gradient at different speeds on the basis of their sizes, shapes, or densities and eventually form different hands in the gradient. Usually, the density gradient is prepared with sucrose, glycerol, cesium chloride, and other aqueous solutions. The advantage of this technique is its nontoxicity. However, for NP prepared in organic medium, transferring from organic solvent to aqueous solution is challenging

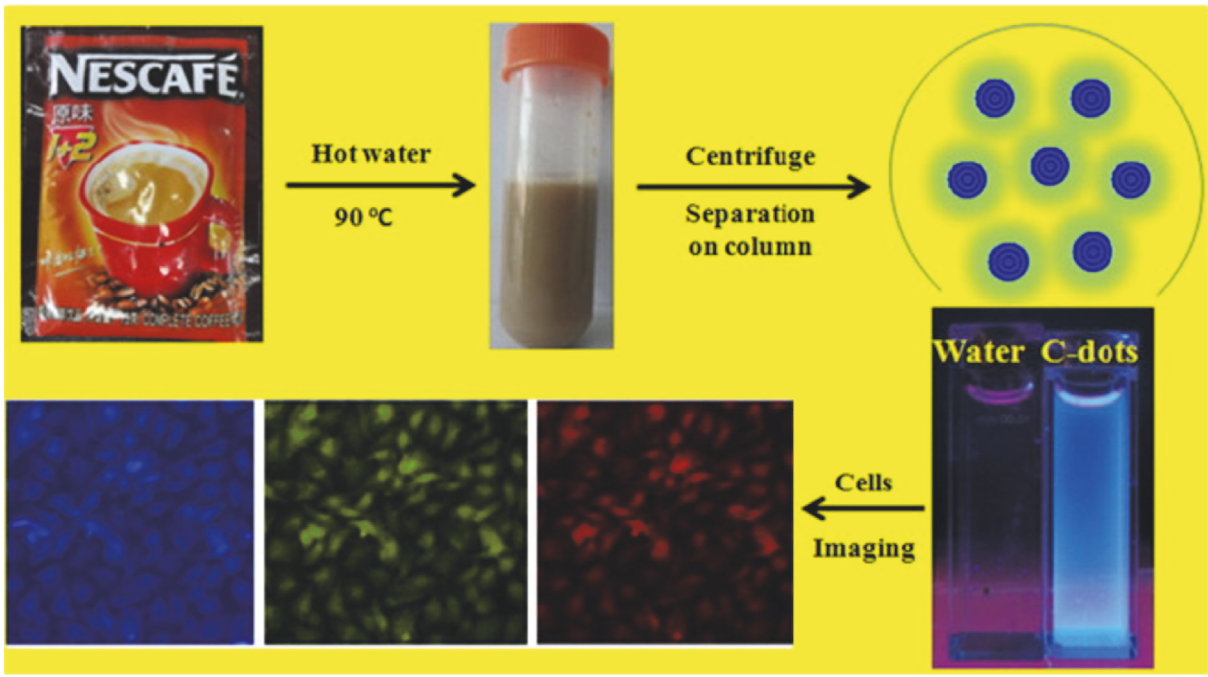

Figure 16: Schematic illustration of the preparation of fluorescent C-dots from Nescafe Original instant coffee by SEC technique and its application for cell imaging [97].

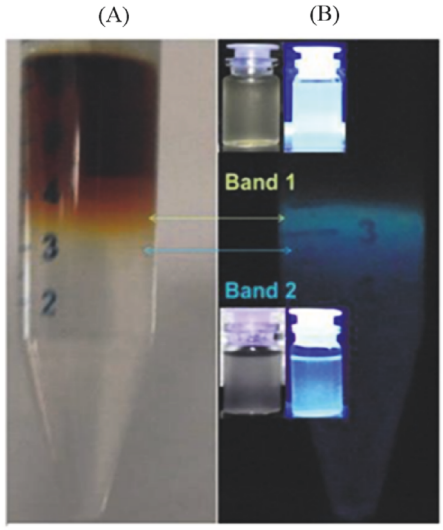

Figure 17: (A) SDGC separation of C-dots from sonication of sugar cane juice. (B) The images of the separated C-dots bands under ambient and UV light [29].

due to the coagulation possibility of some particles [189]. Fortunately, this is not a big problem for C-dots sample which is usually synthesized in aqueous medium and possesses excellent water solubility. Pandey et al. [29] proposed the sucrose density gradient centrifugation (SDGC) method to separate C-dots from other carbonaceous materials. The sample mixture was fractionated in a density gradient formed by overlaying 50–100% of pure sucrose in test tube. Figure 17 shows that fine separation can be achieved based on the size of C-dots species. The obtained fractions exhibited green and blue fluorescence under UV light.

3.4. Differential Centrifugation. Differential centrifugation is used to separate the multiple fractions within a NP sample by size and density; the larger and denser NP precipitate at lower centrifugal forces while the smaller and lighter NP remain in the supernatant and require more force and greater times to precipitate [98]. In a typical differential centrifugation process, a NP mixture is centrifuged multiple times, and after each run the precipitate is removed while the supernatant is centrifuged at a higher centrifugal force. Sahu et al. [98] for the first time reported the use of differential centrifugation method to obtain different size-range C-dots species synthesized by hydrothermal treatment of orange juice (Figure 18). In the centrifugation procedure, the aqueous brown solution containing C-dots was firstly centrifuged at 3000 rpm for 15 min to get the less-fluorescent deposit coarse nanoparticles (CP). Then, an excess amount of acetone was added to the upper brown solution and centrifuged at a high speed of 10,000 rpm for 15 min. The supernatant containing the highly fluorescent nanoparticles (CD) has an average size of 1.5–4.5 nm. The deposit CP exhibiting weak fluorescence have larger size in the range of 30–50 nm.

3.5. Solvent Extraction Process. Solvent extraction, also known as liquid–liquid extraction or partitioning, is a method used to separate a compound based on its solubility in two liquids that do not mix (e.g., water and an organic solvent). This method has been widely used in the isolation

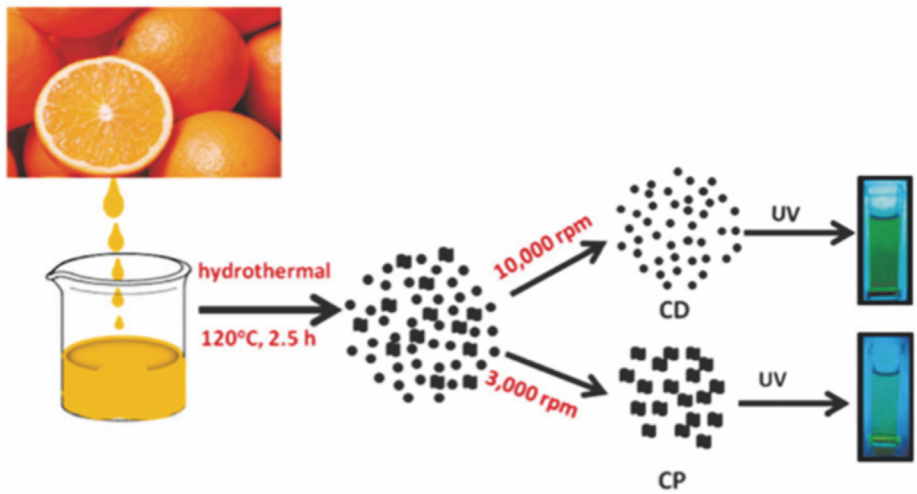

Figure 18: Schematic illustration of the formation and the differential centrifugation of C-dots from hydrothermal treatment of orange juice [98].

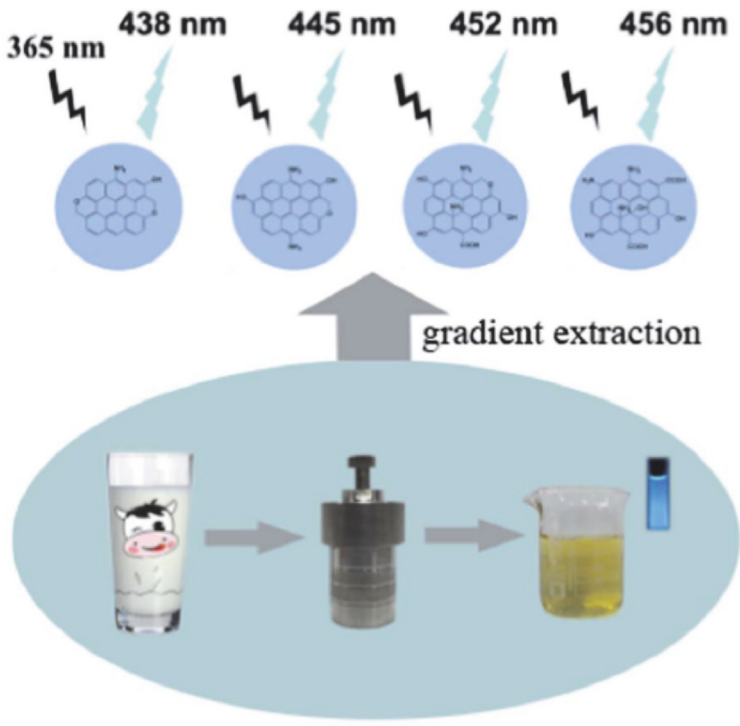

Figure 19: Schematic illustration of the fabrication, gradient extraction, and surface polarity-dependent PL of C-dots [99].

of C-dots from the reaction mixtures. Typically, organic solvents (e.g., ethyl acetate, acetone, chloroform, toluene, and *n*-hexane) are used to extract the amphiphilic C-dots and eliminate unreacted reagents in aqueous solution [111–113]. Recently, Han et al. [99] proposed a novel "gradient extraction" method to separate C-dots synthesized from hydrothermal treatment of cow milk based on their surface polarity of the C-dots species (Figure 19). Four organic solvents with different polarities: hexane (polarity: 0.06), carbon tetrachloride (polarity: 1.6), mixture of carbon tetrachloride and dichloromethane (v/v = 3 : 2), and dichloromethane (polarity: 3.4), were used to extract C-dots fractions. The

four fractions obtained were determined to have different surface polarities and show surface polarity-dependent photoluminescence. The solvent extraction process is certainly good in roughly isolating C-dots from the reaction mixtures; however, it does not possess the ability to completely separate and exactly examine the hidden properties of each individual C-dots species.

3.6. Dialysis. Dialysis is a widely used purification method to separate the C-dots from the potential small fluorescent molecules that can be byproducts of the synthetic route [20, 21, 87, 98, 114, 115]. The dialysis process works on the principles of the diffusion of small fluorescent molecules across a semipermeable membrane based on the principle that the substances in water tend to move from an area of high concentration to an area of low concentration. Usually, the as-synthesized fluorescent product was dissolved in distilled water and dialyzed against a semipermeable membrane in purified water with stirring and recharging with fresh distilled water at different time intervals over a certain time period. The purification by dialysis is certainly very useful to remove the potential small fluorescent species from C-dots sample. However, similar to the solvent extraction process, it is not capable of efficiently separating each individual C-dots species.

4. Conclusion and Outlook

In this review, we outline the general approaches for the characterization and analytical separation of C-dots. Given the complexity of C-dots components and the inherent drawbacks of each technique, only one technique is not enough to capture the complete picture of the C-dots properties. For most of time, multiple characterization and analytical separation techniques described here are used in complementary ways. Though significant progress has been made in recent years, we are still far from achieving full understanding of C-dots properties. Bearing this in mind, much effort is required. On one hand, despite the size and chemical structure of C-dots having been estimated by a number of researchers, the exact molecular weight of C-dots still remains debated, and, therefore, developing new methods with improved resolution and sensitivity based on new or original concepts is essential to progress the characterization of C-dots. On the other hand, carefully checking and refining the existing methods to overcome the limitations and to further improve their working efficiency is of equal importance. While any tiny improvement may not significantly matter, the cumulative effects of a series of such advances will make a substantial change. Furthermore, among the numerous techniques applied to separate or to characterize C-dots, efforts have been seldom used in coupled ways. It is anticipated that the coupled techniques could be further explored in the near future to achieve integrative separation-characterization of C-dots in an efficient way.

Disclosure

Qin Hu's present address is Department of Chemistry, State University of New York at Buffalo, Natural Science Complex, Buffalo, NY 14260, USA. Martin M. F. Choi's present address is Acadia Divinity College, Acadia University, 15 University Avenue, Wolfville, NS, Canada B4P 2R6.

Conflicts of Interest

The authors have declared no conflicts of interest.

Acknowledgments

Financial supports from the HKBU Faculty Research Grant (FRG1/13-14/039), Overseas, Hong Kong and Macau Young Scholars Collaborative Research Fund (41328005), and National Science Foundation of China (21305082) are gratefully acknowledged. Qin Hu acknowledges the receipt of a postgraduate studentship from the University Grants Committee of the Hong Kong Special Administrative Region.

References

[1] Z. Wang and L. Ma, "Gold nanoparticle probes," *Coordination Chemistry Reviews*, vol. 253, no. 11-12, pp. 1607–1618, 2009.

[2] X. Xu, R. Ray, Y. Gu et al., "Electrophoretic analysis and purification of fluorescent single-walled carbon nanotube fragments," *Journal of the American Chemical Society*, vol. 126, no. 40, pp. 12736-12737, 2004.

[3] Q.-L. Zhao, Z.-L. Zhang, B.-H. Huang, J. Peng, M. Zhang, and D.-W. Pang, "Facile preparation of low cytotoxicity fluorescent carbon nanocrystals by electrooxidation of graphite," *Chemical Communications*, no. 41, pp. 5116–5118, 2008.

[4] L. Zheng, Y. Chi, Y. Dong, J. Lin, and B. Wang, "Electrochemiluminescence of water-soluble carbon nanocrystals released electrochemically from graphite," *Journal of the American Chemical Society*, vol. 131, no. 13, pp. 4564-4565, 2009.

[5] J. Zhou, C. Booker, R. Li et al., "An electrochemical avenue to blue luminescent nanocrystals from multiwalled carbon nanotubes (MWCNTs)," *Journal of the American Chemical Society*, vol. 129, no. 4, pp. 744-745, 2007.

[6] S.-L. Hu, K.-Y. Niu, J. Sun, J. Yang, N.-Q. Zhao, and X.-W. Du, "One-step synthesis of fluorescent carbon nanoparticles by laser irradiation," *Journal of Materials Chemistry*, vol. 19, no. 4, pp. 484–488, 2009.

[7] Y.-P. Sun, B. Zhou, Y. Lin et al., "Quantum-sized carbon dots for bright and colorful photoluminescence," *Journal of the American Chemical Society*, vol. 128, no. 24, pp. 7756-7757, 2006.

[8] X. Wang, L. Cao, F. Lu et al., "Photoinduced electron transfers with carbon dots," *Chemical Communications*, no. 25, pp. 3774–3776, 2009.

[9] S.-T. Yang, X. Wang, H. Wang et al., "Carbon dots as nontoxic and high-performance fluorescence imaging agents," *The Journal of Physical Chemistry C*, vol. 113, no. 42, pp. 18110–18114, 2009.

[10] R.-J. Fan, Q. Sun, L. Zhang, Y. Zhang, and A.-H. Lu, "Photoluminescent carbon dots directly derived from polyethylene glycol and their application for cellular imaging," *Carbon*, vol. 71, pp. 87–93, 2014.

[11] B. Zhang, C.-Y. Liu, and Y. Liu, "A novel one-step approach to synthesize fluorescent carbon nanoparticles," *European Journal of Inorganic Chemistry*, no. 28, pp. 4411–4414, 2010.

[12] D. Pan, J. Zhang, Z. Li, and M. Wu, "Hydrothermal route for cutting graphene sheets into blue-luminescent graphene quantum dots," *Advanced Materials*, vol. 22, no. 6, pp. 734–738, 2010.

[13] Z.-C. Yang, M. Wang, A. M. Yong et al., "Intrinsically fluorescent carbon dots with tunable emission derived from hydrothermal treatment of glucose in the presence of monopotassium phosphate," *Chemical Communications*, vol. 47, no. 42, pp. 11615–11617, 2011.

[14] Y. Jiang, Q. Han, C. Jin, J. Zhang, and B. Wang, "A fluorescence turn-off chemosensor based on N-doped carbon quantum dots for detection of Fe3+ in aqueous solution," *Materials Letters*, vol. 141, pp. 366–368, 2015.

[15] A. Barati, M. Shamsipur, E. Arkan, L. Hosseinzadeh, and H. Abdollahi, "Synthesis of biocompatible and highly photoluminescent nitrogen doped carbon dots from lime: Analytical applications and optimization using response surface methodology," *Materials Science and Engineering C*, vol. 47, pp. 325–332, 2015.

[16] A. B. Bourlinos, A. Stassinopoulos, D. Anglos, R. Zboril, M. Karakassides, and E. P. Giannelis, "Surface functionalized carbogenic quantum dots," *Small*, vol. 4, no. 4, pp. 455–458, 2008.

[17] A. B. Bourlinos, A. Stassinopoulos, D. Anglos, R. Zboril, V. Georgakilas, and E. P. Giannelis, "Photoluminescent carbogenic dots," *Chemistry of Materials*, vol. 20, no. 14, pp. 4539–4541, 2008.

[18] P.-C. Hsu and H.-T. Chang, "Synthesis of high-quality carbon nanodots from hydrophilic compounds: Role of functional groups," *Chemical Communications*, vol. 48, no. 33, pp. 3984–3986, 2012.

[19] X. W. Tan, A. N. B. Romainor, S. F. Chin, and S. M. Ng, "Carbon dots production via pyrolysis of sago waste as potential probe for metal ions sensing," *Journal of Analytical and Applied Pyrolysis*, vol. 105, pp. 157–165, 2014.

[20] X. Zhai, P. Zhang, C. Liu et al., "Highly luminescent carbon nanodots by microwave-assisted pyrolysis," *Chemical Communications*, vol. 48, no. 64, pp. 7955–7957, 2012.

[21] S. J. Zhu, Q. N. Meng, L. H. Wang et al., "Highly photoluminescent carbon dots for multicolor patterning, sensors, and bioimaging," *Angewandte Chemie—International Edition*, vol. 52, no. 14, pp. 3953–3957, 2013.

[22] Q. Wang, H. Zheng, Y. Long, L. Zhang, M. Gao, and W. Bai, "Microwave-hydrothermal synthesis of fluorescent carbon dots from graphite oxide," *Carbon*, vol. 49, no. 9, pp. 3134–3140, 2011.

[23] Y. Liu, N. Xiao, N. Gong et al., "One-step microwave-assisted polyol synthesis of green luminescent carbon dots as optical nanoprobes," *Carbon*, vol. 68, pp. 258–264, 2014.

[24] R. Liu, J. Zhang, M. Gao et al., "A facile microwave-hydrothermal approach towards highly photoluminescent carbon dots from goose feathers," *RSC Advances*, vol. 5, no. 6, pp. 4428–4433, 2015.

[25] H. Zhu, X. Wang, Y. Li, Z. Wang, F. Yang, and X. Yang, "Microwave synthesis of fluorescent carbon nanoparticles with electrochemiluminescence properties," *Chemical Communications*, no. 34, pp. 5118–5120, 2009.

[26] X. Qin, W. Lu, A. M. Asiri, A. O. Al-Youbi, and X. Sun, "Green, low-cost synthesis of photoluminescent carbon dots by hydrothermal treatment of willow bark and their application as an effective photocatalyst for fabricating Au nanoparticles-reduced graphene oxide nanocomposites for glucose detection," *Catalysis Science and Technology*, vol. 3, no. 4, pp. 1027–1035, 2013.

[27] J. Wang, C.-F. Wang, and S. Chen, "Amphiphilic egg-derived carbon dots: rapid plasma fabrication, pyrolysis process, and multicolor printing patterns," *Angewandte Chemie—International Edition*, vol. 51, no. 37, pp. 9297–9301, 2012.

[28] X.-M. Wei, Y. Xu, Y.-H. Li, X.-B. Yin, and X.-W. He, "Ultrafast synthesis of nitrogen-doped carbon dots via neutralization heat for bioimaging and sensing applications," *RSC Advances*, vol. 4, no. 84, pp. 44504–44508, 2014.

[29] S. Pandey, A. Mewada, G. Oza et al., "Synthesis and centrifugal separation of fluorescent carbon dots at room temperature," *Nanoscience and Nanotechnology Letters*, vol. 5, no. 7, pp. 775–779, 2013.

[30] Z. Zhang, J. Hao, J. Zhang, B. Zhang, and J. Tang, "Protein as the source for synthesizing fluorescent carbon dots by a one-pot hydrothermal route," *RSC Advances*, vol. 2, no. 23, pp. 8599–8601, 2012.

[31] Z. L. Wu, P. Zhang, M. X. Gao et al., "One-pot hydrothermal synthesis of highly luminescent nitrogen-doped amphoteric carbon dots for bioimaging from Bombyx mori silk-natural proteins," *Journal of Materials Chemistry B*, vol. 1, no. 22, pp. 2868–2873, 2013.

[32] A. Mewada, S. Pandey, S. Shinde et al., "Green synthesis of biocompatible carbon dots using aqueous extract of Trapa bispinosa peel," *Materials Science and Engineering C*, vol. 33, no. 5, pp. 2914–2917, 2013.

[33] D. Sun, R. Ban, P.-H. Zhang, G.-H. Wu, J.-R. Zhang, and J.-J. Zhu, "Hair fiber as a precursor for synthesizing of sulfur- and nitrogen-co-doped carbon dots with tunable luminescence properties," *Carbon*, vol. 64, pp. 424–434, 2013.

[34] S. Yang, J. Sun, X. Li et al., "Large-scale fabrication of heavy doped carbon quantum dots with tunable-photoluminescence and sensitive fluorescence detection," *Journal of Materials Chemistry A*, vol. 2, no. 23, pp. 8660–8667, 2014.

[35] S. Y. Park, H. U. Lee, E. S. Park et al., "Photoluminescent green carbon nanodots from food-waste-derived sources: large-scale synthesis, properties, and biomedical applications," *ACS Applied Materials & Interfaces*, vol. 6, no. 5, pp. 3365–3370, 2014.

[36] X. Teng, C. Ma, C. Ge et al., "Green synthesis of nitrogen-doped carbon dots from konjac flour with "off-on" fluorescence by Fe3+ and l-lysine for bioimaging," *Journal of Materials Chemistry B*, vol. 2, no. 29, pp. 4631–4639, 2014.

[37] L. Wang and H. S. Zhou, "Green synthesis of luminescent nitrogen-doped carbon dots from milk and its imaging application," *Analytical Chemistry*, vol. 86, no. 18, pp. 8902–8905, 2014.

[38] Z.-Q. Xu, L.-Y. Yang, X.-Y. Fan et al., "Low temperature synthesis of highly stable phosphate functionalized two color carbon nanodots and their application in cell imaging," *Carbon*, vol. 66, pp. 351–360, 2014.

[39] Y. Li, X. Zhong, A. E. Rider, S. A. Furman, and K. Ostrikov, "Fast, energy-efficient synthesis of luminescent carbon quantum dots," *Green Chemistry*, vol. 16, no. 5, pp. 2566–2570, 2014.

[40] Y. Fang, S. Guo, D. Li et al., "Easy synthesis and imaging applications of cross-linked green fluorescent hollow carbon nanoparticles," *ACS Nano*, vol. 6, no. 1, pp. 400–409, 2012.

[41] J. Niu, H. Gao, L. Wang et al., "Facile synthesis and optical properties of nitrogen-doped carbon dots," *New Journal of Chemistry*, vol. 38, no. 4, pp. 1522–1527, 2014.

[42] H. Zhang, Y. Chen, M. Liang et al., "Solid-phase synthesis of highly fluorescent nitrogen-doped carbon dots for sensitive and selective probing ferric ions in living cells," *Analytical Chemistry*, vol. 86, no. 19, pp. 9846–9852, 2014.

[43] L. Wang, Y. Yin, A. Jain, and H. Susan Zhou, "Aqueous phase synthesis of highly luminescent, nitrogen-doped carbon dots and their application as bioimaging agents," *Langmuir*, vol. 30, no. 47, pp. 14270–14275, 2014.

[44] H. Huang, C. Li, S. Zhu et al., "Histidine-derived nontoxic nitrogen-doped carbon dots for sensing and bioimaging applications," *Langmuir*, vol. 30, no. 45, pp. 13542–13548, 2014.

[45] M. Xu, G. He, Z. Li et al., "A green heterogeneous synthesis of N-doped carbon dots and their photoluminescence applications in solid and aqueous states," *Nanoscale*, vol. 6, no. 17, pp. 10307–10315, 2014.

[46] W. Wang, Y.-C. Lu, H. Huang, A.-J. Wang, J.-R. Chen, and J.-J. Feng, "Solvent-free synthesis of sulfur- and nitrogen-co-doped fluorescent carbon nanoparticles from glutathione for highly selective and sensitive detection of mercury(II) ions," *Sensors and Actuators, B: Chemical*, vol. 202, pp. 741–747, 2014.

[47] Y. Dong, H. Pang, H. B. Yang et al., "Carbon-based dots co-doped with nitrogen and sulfur for high quantum yield and excitation-independent emission," *Angewandte Chemie - International Edition*, vol. 52, no. 30, pp. 7800–7804, 2013.

[48] D. Wang, X. Wang, Y. Guo, W. Liu, and W. Qin, "Luminescent properties of milk carbon dots and their sulphur and nitrogen doped analogues," *RSC Advances*, vol. 4, no. 93, pp. 51658–51665, 2014.

[49] C. Wang, D. Sun, K. Zhuo, H. Zhang, and J. Wang, "Simple and green synthesis of nitrogen-, sulfur-, and phosphorus-co-doped carbon dots with tunable luminescence properties and sensing application," *RSC Advances*, vol. 4, no. 96, pp. 54060–54065, 2014.

[50] Y. Zou, F. Yan, T. Zheng et al., "Highly luminescent organosilane-functionalized carbon dots as a nanosensor for sensitive and selective detection of quercetin in aqueous solution," *Talanta*, vol. 135, pp. 145–148, 2015.

[51] H. Liu, T. Ye, and C. Mao, "Fluorescent carbon nanoparticles derived from candle soot," *Angewandte Chemie International Edition*, vol. 46, no. 34, pp. 6473–6475, 2007.

[52] S. N. Baker and G. A. Baker, "Luminescent carbon nanodots: emergent nanolights," *Angewandte Chemie*, vol. 49, no. 38, pp. 6726–6744, 2010.

[53] Z. Yang, Z. Li, M. Xu et al., "Controllable synthesis of fluorescent carbon dots and their detection application as nanoprobes," *Nano-Micro Letters*, vol. 5, no. 4, pp. 247–259, 2013.

[54] L. Cao, X. Wang, M. J. Meziani et al., "Carbon dots for multiphoton bioimaging," *Journal of the American Chemical Society*, vol. 129, no. 37, pp. 11318-11319, 2007.

[55] S.-T. Yang, L. Cao, P. G. Luo et al., "Carbon dots for optical imaging *in vivo*," *Journal of the American Chemical Society*, vol. 131, no. 32, pp. 11308-11309, 2009.

[56] K. Qu, J. Wang, J. Ren, and X. Qu, "Carbon dots prepared by hydrothermal treatment of dopamine as an effective fluorescent sensing platform for the label-free detection of iron(III) ions and dopamine," *Chemistry*, vol. 19, no. 22, pp. 7243–7249, 2013.

[57] Z. Lin, X. Dou, H. Li, Y. Ma, and J.-M. Lin, "Nitrite sensing based on the carbon dots-enhanced chemiluminescence from peroxynitrous acid and carbonate," *Talanta*, vol. 132, pp. 457–462, 2015.

[58] H. Gonçalves, P. A. S. Jorge, J. R. A. Fernandes, and J. C. G. Esteves da Silva, "Hg(II) sensing based on functionalized carbon dots obtained by direct laser ablation," *Sensors and Actuators, B: Chemical*, vol. 145, no. 2, pp. 702–707, 2010.

[59] P. Zhang, Z. Xue, D. Luo, W. Yu, Z. Guo, and T. Wang, "Dual-Peak electrogenerated chemiluminescence of carbon dots for iron ions detection," *Analytical Chemistry*, vol. 86, no. 12, pp. 5620–5623, 2014.

[60] I. Costas-Mora, V. Romero, I. Lavilla, and C. Bendicho, "In situ building of a nanoprobe based on fluorescent carbon dots for methylmercury detection," *Analytical Chemistry*, vol. 86, no. 9, pp. 4536–4543, 2014.

[61] A. Zhao, C. Zhao, M. Li, J. Ren, and X. Qu, "Ionic liquids as precursors for highly luminescent, surface-different nitrogen-doped carbon dots used for label-free detection of Cu2+/Fe3+ and cell imaging," *Analytica Chimica Acta*, vol. 809, pp. 128–133, 2014.

[62] J. Zong, X. Yang, A. Trinchi et al., "Carbon dots as fluorescent probes for 'off-on' detection of Cu^{2+} and l-cysteine in aqueous solution," *Biosensors & Bioelectronics*, vol. 51, pp. 330–335, 2014.

[63] Y. Liu, C.-Y. Liu, and Z.-Y. Zhang, "Synthesis of highly luminescent graphitized carbon dots and the application in the Hg2+ detection," *Applied Surface Science*, vol. 263, pp. 481–485, 2012.

[64] J. Xu, Y. Zhou, S. Liu, M. Dong, and C. Huang, "Low-cost synthesis of carbon nanodots from natural products used as a fluorescent probe for the detection of ferrum(iii) ions in lake water," *Analytical Methods*, vol. 6, no. 7, pp. 2086–2090, 2014.

[65] R. H. Liu, H. T. Li, W. Q. Kong et al., "Ultra-sensitive and selective Hg^{2+} detection based on fluorescent carbon dots," *Materials Research Bulletin*, vol. 48, no. 7, pp. 2529–2534, 2013.

[66] L. Zhou, Y. Lin, Z. Huang, J. Ren, and X. Qu, "Carbon nanodots as fluorescence probes for rapid, sensitive, and label-free detection of Hg2+ and biothiols in complex matrices," *Chemical Communications*, vol. 48, no. 8, pp. 1147–1149, 2012.

[67] H. Wang, J. Shen, Y. Li et al., "Magnetic iron oxide-fluorescent carbon dots integrated nanoparticles for dual-modal imaging, near-infrared light-responsive drug carrier and photothermal therapy," *Biomaterials Science*, vol. 2, no. 6, pp. 915–923, 2014.

[68] H. Ding, F. Du, P. Liu, Z. Chen, and J. Shen, "DNA–carbon dots function as fluorescent vehicles for drug delivery," *ACS Applied Materials & Interfaces*, vol. 7, no. 12, pp. 6889–6897, 2015.

[69] T. Feng, X. Ai, G. An, P. Yang, and Y. Zhao, "Charge-Convertible Carbon Dots for Imaging-Guided Drug Delivery with Enhanced in Vivo Cancer Therapeutic Efficiency," *ACS Nano*, vol. 10, no. 4, pp. 4410–4420, 2016.

[70] Q. Zeng, D. Shao, X. He et al., "Carbon dots as a trackable drug delivery carrier for localized cancer therapy: in vivo," *Journal of Materials Chemistry B*, vol. 4, no. 30, pp. 5119–5126, 2016.

[71] M. Zheng, S. Liu, J. Li et al., "Integrating oxaliplatin with highly luminescent carbon dots: an unprecedented theranostic agent for personalized medicine," *Advanced Materials*, vol. 26, no. 21, pp. 3554–3560, 2014.

[72] J. Wang, Z. Zhang, S. Zha et al., "Carbon nanodots featuring efficient FRET for two-photon photodynamic cancer therapy with a low fs laser power density," *Biomaterials*, vol. 35, no. 34, pp. 9372–9381, 2014.

[73] H. Liu, Q. Wang, G. Shen et al., "A multifunctional ribonuclease A-conjugated carbon dot cluster nanosystem for synchronous cancer imaging and therapy," *Nanoscale Research Letters*, vol. 9, no. 1, pp. 1–11, 2014.

[74] Z. M. Markovic, B. Z. Ristic, K. M. Arsikin et al., "Graphene quantum dots as autophagy-inducing photodynamic agents," *Biomaterials*, vol. 33, no. 29, pp. 7084–7092, 2012.

[75] I. L. Christensen, Y.-P. Sun, and P. Juzenas, "Carbon dots as antioxidants and prooxidants," *Journal of Biomedical Nanotechnology*, vol. 7, no. 5, pp. 667–676, 2011.

[76] Q. Liu, B. Guo, Z. Rao, B. Zhang, and J. R. Gong, "Strong two-photon-induced fluorescence from photostable, biocompatible nitrogen-doped graphene quantum dots for cellular and deep-tissue imaging," *Nano Letters*, vol. 13, no. 6, pp. 2436–2441, 2013.

[77] Y. Wang, S. Kalytchuk, L. Wang et al., "Carbon dot hybrids with oligomeric silsesquioxane: Solid-state luminophores with high photoluminescence quantum yield and applicability in white light emitting devices," *Chemical Communications*, vol. 51, no. 14, pp. 2950–2953, 2015.

[78] F. Wang, Y.-H. Chen, C.-Y. Liu, and D.-G. Ma, "White light-emitting devices based on carbon dots' electroluminescence," *Chemical Communications*, vol. 47, no. 12, pp. 3502–3504, 2011.

[79] X. Zhang, Y. Zhang, Y. Wang et al., "Color-switchable electroluminescence of carbon dot light-emitting diodes," *ACS Nano*, vol. 7, no. 12, pp. 11234–11241, 2013.

[80] C.-X. Li, C. Yu, C.-F. Wang, and S. Chen, "Facile plasma-induced fabrication of fluorescent carbon dots toward high-performance white LEDs," *Journal of Materials Science*, vol. 48, no. 18, pp. 6307–6311, 2013.

[81] C. Sun, Y. Zhang, Y. Wang et al., "High color rendering index white light emitting diodes fabricated from a combination of carbon dots and zinc copper indium sulfide quantum dots," *Applied Physics Letters*, vol. 104, no. 26, Article ID 261106, 2014.

[82] H. Choi, S.-J. Ko, Y. Choi et al., "Versatile surface plasmon resonance of carbon-dot-supported silver nanoparticles in polymer optoelectronic devices," *Nature Photonics*, vol. 7, no. 9, pp. 732–738, 2013.

[83] Q. Wang, S. Zhang, H. Ge, G. Tian, N. Cao, and Y. Li, "A fluorescent turn-off/on method based on carbon dots as fluorescent probes for the sensitive determination of Pb^{2+} and pyrophosphate in an aqueous solution," *Sensors and Actuators, B: Chemical*, vol. 207, pp. 25–33, 2015.

[84] W. Chen, C. Hu, Y. Yang, J. Cui, and Y. Liu, "Rapid synthesis of carbon dots by hydrothermal treatment of lignin," *Materials*, vol. 9, no. 3, article no. 184, 2016.

[85] J. J. Huang, Z. F. Zhong, M. Z. Rong, X. Zhou, X. D. Chen, and M. Q. Zhang, "An easy approach of preparing strongly luminescent carbon dots and their polymer based composites for enhancing solar cell efficiency," *Carbon*, vol. 70, pp. 190–198, 2014.

[86] C. Liu, P. Zhang, X. Zhai et al., "Nano-carrier for gene delivery and bioimaging based on carbon dots with PEI-passivation enhanced fluorescence," *Biomaterials*, vol. 33, no. 13, pp. 3604–3613, 2012.

[87] Y. Hu, J. Yang, J. Tian, L. Jia, and J.-S. Yu, "Waste frying oil as a precursor for one-step synthesis of sulfur-doped carbon dots with pH-sensitive photoluminescence," *Carbon*, vol. 77, pp. 775–782, 2014.

[88] A. Khanam, S. K. Tripathi, D. Roy, and M. Nasim, "A facile and novel synthetic method for the preparation of hydroxyl capped fluorescent carbon nanoparticles," *Colloids and Surfaces B: Biointerfaces*, vol. 102, pp. 63–69, 2013.

[89] W. Kong, H. Wu, Z. Ye, R. Li, T. Xu, and B. Zhang, "Optical properties of pH-sensitive carbon-dots with different modifications," *Journal of Luminescence*, vol. 148, pp. 238–242, 2014.

[90] L. Tian, D. Ghosh, W. Chen, S. Pradhan, X. Chang, and S. Chen, "Nanosized carbon particles from natural gas soot," *Chemistry of Materials*, vol. 21, no. 13, pp. 2803–2809, 2009.

[91] Q. Hu, M. C. Paau, M. M. F. Choi et al., "Better understanding of carbon nanoparticles via high-performance liquid chromatography-fluorescence detection and mass spectrometry," *Electrophoresis*, vol. 35, no. 17, pp. 2454–2462, 2014.

[92] Q. Hu, X. Meng, and W. Chan, "An investigation on the chemical structure of nitrogen and sulfur codoped carbon nanoparticles by ultra-performance liquid chromatography-tandem mass spectrometry," *Analytical and Bioanalytical Chemistry*, vol. 408, no. 19, pp. 5347–5357, 2016.

[93] T. J. Bandosz, E. Rodriguez-Castellon, J. M. Montenegro, and M. Seredych, "Photoluminescence of nanoporous carbons: Opening a new application route for old materials," *Carbon*, vol. 77, pp. 651–659, 2014.

[94] Q. Hu, M. C. Paau, Y. Zhang et al., "Capillary electrophoretic study of amine/carboxylic acid-functionalized carbon nanodots," *Journal of Chromatography A*, vol. 1304, pp. 234–240, 2013.

[95] J. C. Vinci and L. A. Colon, "Fractionation of carbon-based nanomaterials by anion-exchange HPLC," *Analytical Chemistry*, vol. 84, no. 2, pp. 1178–1183, 2012.

[96] X. Gong, Q. Hu, M. Chin Paau et al., "High-performance liquid chromatographic and mass spectrometric analysis of fluorescent carbon nanodots," *Talanta*, vol. 129, pp. 529–538, 2014.

[97] C. Jiang, H. Wu, X. Song, X. Ma, J. Wang, and M. Tan, "Presence of photoluminescent carbon dots in Nescafe® original instant coffee: Applications to bioimaging," *Talanta*, vol. 127, pp. 68–74, 2014.

[98] S. Sahu, B. Behera, T. K. Maiti, and S. Mohapatra, "Simple one-step synthesis of highly luminescent carbon dots from orange juice: application as excellent bio-imaging agents," *Chemical Communications*, vol. 48, no. 70, pp. 8835–8837, 2012.

[99] S. Han, H. Zhang, J. Zhang et al., "Fabrication, gradient extraction and surface polarity-dependent photoluminescence of cow milk-derived carbon dots," *RSC Advances*, vol. 4, no. 101, pp. 58084–58089, 2014.

[100] J. C. Vinci, I. M. Ferrer, S. J. Seedhouse et al., "Hidden properties of carbon dots revealed after HPLC fractionation," *Journal of Physical Chemistry Letters*, vol. 4, no. 2, pp. 239–243, 2013.

[101] J. C. Vinci and L. A. Colón, "Surface chemical composition of chromatographically fractionated graphite nanofiber-derived carbon dots," *Microchemical Journal*, vol. 110, pp. 660–664, 2013.

[102] H. Li, J. Liu, M. Yang, W. Kong, H. Huang, and Y. Liu, "Highly sensitive, stable, and precise detection of dopamine with carbon dots/tyrosinase hybrid as fluorescent probe," *RSC Advances*, vol. 4, no. 87, pp. 46437–46443, 2014.

[103] A. Sachdev, I. Matai, and P. Gopinath, "Implications of surface passivation on physicochemical and bioimaging properties of carbon dots," *RSC Advances*, vol. 4, no. 40, pp. 20915–20921, 2014.

[104] J. S. Baker and L. A. Colón, "Influence of buffer composition on the capillary electrophoretic separation of carbon nanoparticles," *Journal of Chromatography A*, vol. 1216, no. 52, pp. 9048–9054, 2009.

[105] M. B. Müller, J. P. Quirino, P. N. Nesterenko et al., "Capillary zone electrophoresis of graphene oxide and chemically converted graphene," *Journal of Chromatography A*, vol. 1217, no. 48, pp. 7593–7597, 2010.

[106] L. Liu, F. Feng, Q. Hu et al., "Capillary electrophoretic study of green fluorescent hollow carbon nanoparticles," *Electrophoresis*, vol. 36, no. 17, pp. 2110–2119, 2015.

[107] Y. Liu, J. Hu, Y. Li et al., "Synthesis of polyethyleneimine capped carbon dots for preconcentration and slurry sampling analysis of trace chromium in environmental water samples," *Talanta*, vol. 134, pp. 16–23, 2015.

[108] X. Gong, Q. Hu, M. C. Paau et al., "Red-green-blue fluorescent hollow carbon nanoparticles isolated from chromatographic fractions for cellular imaging," *Nanoscale*, vol. 6, no. 14, pp. 8162–8170, 2014.

[109] X. Wang, L. Cao, S.-T. Yang et al., "Bandgap-like strong fluorescence in functionalized carbon nanoparticles," *Angewandte Chemie - International Edition*, vol. 49, no. 31, pp. 5310–5314, 2010.

[110] J. D. Robertson, L. Rizzello, M. Avila-Olias et al., "Purification of Nanoparticles by Size and Shape," *Scientific Reports*, vol. 6, Article ID 27494, 2016.

[111] S. Mitra, S. Chandra, T. Kundu, R. Banerjee, P. Pramanik, and A. Goswami, "Rapid microwave synthesis of fluorescent hydrophobic carbon dots," *RSC Advances*, vol. 2, no. 32, pp. 12129–12131, 2012.

[112] J. F. Y. Fong, S. F. Chin, and S. M. Ng, "Facile synthesis of carbon nanoparticles from sodium alginate via ultrasonic-assisted nano-precipitation and thermal acid dehydration for ferric ion sensing," *Sensors and Actuators B: Chemical*, vol. 209, pp. 997–1004, 2015.

[113] H. M. R. Gonçalves, A. J. Duarte, and J. C. G. Esteves da Silva, "Optical fiber sensor for Hg(II) based on carbon dots," *Biosensors & Bioelectronics*, vol. 26, no. 4, pp. 1302–1306, 2010.

[114] A. B. Bourlinos, G. Trivizas, M. A. Karakassides et al., "Green and simple route toward boron doped carbon dots with significantly enhanced non-linear optical properties," *Carbon*, vol. 83, pp. 173–179, 2015.

[115] L. Hu, Y. Sun, S. Li et al., "Multifunctional carbon dots with high quantum yield for imaging and gene delivery," *Carbon*, vol. 67, pp. 508–513, 2014.

[116] H. Li, Z. Kang, Y. Liu, and S.-T. Lee, "Carbon nanodots: synthesis, properties and applications," *Journal of Materials Chemistry*, vol. 22, no. 46, pp. 24230–24253, 2012.

[117] C. Ding, A. Zhu, and Y. Tian, "Functional surface engineering of C-dots for fluorescent biosensing and in vivo bioimaging," *Accounts of Chemical Research*, vol. 47, no. 1, pp. 20–30, 2014.

[118] A. Zhao, Z. Chen, C. Zhao, N. Gao, J. Ren, and X. Qu, "Recent advances in bioapplications of C-dots," *Carbon*, vol. 85, pp. 309–327, 2015.

[119] S. Zhang, Q. Wang, G. Tian, and H. Ge, "A fluorescent turn-off/on method for detection of Cu2+and oxalate using carbon dots as fluorescent probes in aqueous solution," *Materials Letters*, vol. 115, pp. 233–236, 2014.

[120] J. Liu, J. Yu, J. Chen, R. Yang, and K. Shih, "Signal-amplification and real-time fluorescence anisotropy detection of apyrase by carbon nanoparticle," *Materials Science and Engineering C*, vol. 38, no. 1, pp. 206–211, 2014.

[121] C. Wang, Z. Xu, H. Cheng, H. Lin, M. G. Humphrey, and C. Zhang, "A hydrothermal route to water-stable luminescent carbon dots as nanosensors for pH and temperature," *Carbon*, vol. 82, no. C, pp. 87–95, 2015.

[122] X. Qin, W. Lu, A. M. Asiri, A. O. Al-Youbi, and X. Sun, "Microwave-assisted rapid green synthesis of photoluminescent carbon nanodots from flour and their applications for sensitive and selective detection of mercury(II) ions," *Sensors and Actuators, B: Chemical*, vol. 184, pp. 156–162, 2013.

[123] C. Gommes, S. Blacher, K. Masenelli-Varlot et al., "Image analysis characterization of multi-walled carbon nanotubes," *Carbon*, vol. 41, no. 13, pp. 2561–2572, 2003.

[124] Ch. Täschner, F. Pácal, A. Leonhardt et al., "Synthesis of aligned carbon nanotubes by DC plasma-enhanced hot filament CVD," *Surface and Coatings Technology*, vol. 174-175, pp. 81–87, 2003.

[125] Z. Gao, G. Shen, X. Zhao et al., "Carbon dots: a safe nanoscale substance for the immunologic system of mice," *Nanoscale Research Letters*, vol. 8, no. 1, article 276, 2013.

[126] H. Dai, Y. Shi, Y. Wang et al., "A carbon dot based biosensor for melamine detection by fluorescence resonance energy transfer," *Sensors and Actuators, B: Chemical*, vol. 202, pp. 201–208, 2014.

[127] W. Wang, T. Kim, Z. Yan et al., "Carbon dots functionalized by organosilane with double-sided anchoring for nanomolar Hg2+ detection," *Journal of Colloid and Interface Science*, vol. 437, pp. 28–34, 2015.

[128] X. Gao, C. Ding, A. Zhu, and Y. Tian, "Carbon-dot-based ratiometric fluorescent probe for imaging and biosensing of superoxide anion in live cells," *Analytical Chemistry*, vol. 86, no. 14, pp. 7071–7078, 2014.

[129] K. Tiede, S. P. Tear, H. David, and A. B. A. Boxall, "Imaging of engineered nanoparticles and their aggregates under fully liquid conditions in environmental matrices," *Water Research*, vol. 43, no. 13, pp. 3335–3343, 2009.

[130] L. Zhou, B. He, and J. Huang, "Amphibious fluorescent carbon dots: One-step green synthesis and application for light-emitting polymer nanocomposites," *Chemical Communications*, vol. 49, no. 73, pp. 8078–8080, 2013.

[131] S. F. Chin, S. N. A. M. Yazid, S. C. Pang, and S. M. Ng, "Facile synthesis of fluorescent carbon nanodots from starch nanoparticles," *Materials Letters*, vol. 85, pp. 50–52, 2012.

[132] M. Zheng, Z. G. Xie, D. Qu et al., "On-off-on fluorescent carbon dot nanosensor for recognition of chromium(VI) and ascorbic acid based on the inner filter effect," *ACS Applied Materials and Interfaces*, vol. 5, no. 24, pp. 13242–13247, 2013.

[133] J. Gong, X. An, and X. Yan, "A novel rapid and green synthesis of highly luminescent carbon dots with good biocompatibility for cell imaging," *New Journal of Chemistry*, vol. 38, no. 4, pp. 1376–1379, 2014.

[134] X. Jin, X. Sun, G. Chen et al., "PH-sensitive carbon dots for the visualization of regulation of intracellular pH inside living pathogenic fungal cells," *Carbon*, vol. 81, no. 1, pp. 388–395, 2015.

[135] L.-H. Mao, W.-Q. Tang, Z.-Y. Deng, S.-S. Liu, C.-F. Wang, and S. Chen, "Facile access to white fluorescent carbon dots toward light-emitting devices," *Industrial & Engineering Chemistry Research*, vol. 53, no. 15, pp. 6417–6425, 2014.

[136] V. N. Mehta, S. Jha, and S. K. Kailasa, "One-pot green synthesis of carbon dots by using *Saccharum officinarum* juice for fluorescent imaging of bacteria (*Escherichia coli*) and yeast (*Saccharomyces cerevisiae*) cells," *Materials Science & Engineering C*, vol. 38, no. 1, pp. 20–27, 2014.

[137] H. Kato, M. Suzuki, K. Fujita et al., "Reliable size determination of nanoparticles using dynamic light scattering method for in vitro toxicology assessment," *Toxicology in Vitro*, vol. 23, no. 5, pp. 927–934, 2009.

[138] H. Kato, A. Nakamura, K. Takahashi, and S. Kinugasa, "Accurate size and size-distribution determination of polystyrene latex nanoparticles in aqueous medium using dynamic light scattering and asymmetrical flow field flow fractionation with multi-angle light scattering," *Nanomaterials*, vol. 2, no. 1, pp. 15–30, 2012.

[139] T. H. Kim, F. Wang, P. McCormick, L. Wang, C. Brown, and Q. Li, "Salt-embedded carbon nanodots as a UV and thermal stable fluorophore for light-emitting diodes," *Journal of Luminescence*, vol. 154, pp. 1–7, 2014.

[140] P.-C. Chen, Y.-N. Chen, P.-C. Hsu, C.-C. Shih, and H.-T. Chang, "Photoluminescent organosilane-functionalized carbon dots as

temperature probes," *Chemical Communications*, vol. 49, no. 16, pp. 1639–1641, 2013.

[141] Z. Lin, X. Dou, H. Li, Q. Chen, and J.-M. Lin, "Silicon-hybrid carbon dots strongly enhance the chemiluminescence of luminol," *Microchimica Acta*, vol. 181, no. 7-8, pp. 805–811, 2014.

[142] P. Shen and Y. Xia, "Synthesis-modification integration: One-step fabrication of boronic acid functionalized carbon dots for fluorescent blood sugar sensing," *Analytical Chemistry*, vol. 86, no. 11, pp. 5323–5329, 2014.

[143] G. H. G. Ahmed, R. B. Laíño, J. A. G. Calzón, and M. E. D. García, "Fluorescent carbon nanodots for sensitive and selective detection of tannic acid in wines," *Talanta*, vol. 132, pp. 252–257, 2015.

[144] Z.-A. Qiao, Y. Wang, Y. Gao et al., "Commercially activated carbon as the source for producing multicolor photoluminescent carbon dots by chemical oxidation," *Chemical Communications*, vol. 46, no. 46, pp. 8812–8814, 2010.

[145] Y. Xu, M. Wu, X.-Z. Feng, X.-B. Yin, X.-W. He, and Y.-K. Zhang, "Reduced carbon dots versus oxidized carbon dots: Photo- and electrochemiluminescence investigations for selected applications," *Chemistry - A European Journal*, vol. 19, no. 20, pp. 6282–6288, 2013.

[146] X. J. Zhao, W. L. Zhang, and Z. Q. Zhou, "Sodium hydroxide-mediated hydrogel of citrus pectin for preparation of fluorescent carbon dots for bioimaging," *Colloids and Surfaces B: Biointerfaces*, vol. 123, pp. 493–497, 2014.

[147] A. Talib, S. Pandey, M. Thakur, and H.-F. Wu, "Synthesis of highly fluorescent hydrophobic carbon dots by hot injection method using Paraplast as precursor," *Materials Science and Engineering C*, vol. 48, pp. 700–703, 2015.

[148] J. J. Zhou, Z. H. Sheng, H. Y. Han, M. Q. Zou, and C. X. Li, "Facile synthesis of fluorescent carbon dots using watermelon peel as a carbon source," *Materials Letters*, vol. 66, no. 1, pp. 222–224, 2012.

[149] A. Cayuela, M. L. Soriano, M. C. Carrión, and M. Valcárcel, "Functionalized carbon dots as sensors for gold nanoparticles in spiked samples: Formation of nanohybrids," *Analytica Chimica Acta*, vol. 820, pp. 133–138, 2014.

[150] J. Wei, X. Zhang, Y. Sheng et al., "Dual functional carbon dots derived from cornflour via a simple one-pot hydrothermal route," *Materials Letters*, vol. 123, pp. 107–111, 2014.

[151] Y. Guo and B. Li, "Carbon dots-initiated luminol chemiluminescence in the absence of added oxidant," *Carbon*, vol. 82, no. C, pp. 459–469, 2015.

[152] F. Wang, S. Pang, L. Wang, Q. Li, M. Kreiter, and C.-Y. Liu, "One-step synthesis of highly luminescent carbon dots in noncoordinating solvents," *Chemistry of Materials*, vol. 22, no. 16, pp. 4528–4530, 2010.

[153] L. Wang, F. Ruan, T. Lv et al., "One step synthesis of Al/N co-doped carbon nanoparticles with enhanced photoluminescence," *Journal of Luminescence*, vol. 158, pp. 1–5, 2015.

[154] F. Li, C. Liu, J. Yang, Z. Wang, W. Liu, and F. Tian, "Mg/N double doping strategy to fabricate extremely high luminescent carbon dots for bioimaging," *RSC Advances*, vol. 4, no. 7, pp. 3201–3205, 2014.

[155] Y. Guo, D. Wang, X. Liu, X. Wang, W. Liu, and W. Qin, "Synthesis and characterization of the nickel@carbon dots hybrid material and its application in the reduction of Cr(vi)," *New Journal of Chemistry*, vol. 38, no. 12, pp. 5861–5867, 2014.

[156] C. Herrero-Latorre, J. Álvarez-Méndez, J. Barciela-García, S. García-Martín, and R. M. Peña-Crecente, "Characterization of carbon nanotubes and analytical methods for their determination in environmental and biological samples: a review," *Analytica Chimica Acta*, vol. 853, no. 1, pp. 77–94, 2015.

[157] B. De and N. Karak, "A green and facile approach for the synthesis of water soluble fluorescent carbon dots from banana juice," *RSC Advances*, vol. 3, no. 22, pp. 8286–8290, 2013.

[158] S. Pandey, A. Mewada, M. Thakur, A. Tank, and M. Sharon, "Cysteamine hydrochloride protected carbon dots as a vehicle for the efficient release of the anti-schizophrenic drug haloperidol," *RSC Advances*, vol. 3, no. 48, pp. 26290–26296, 2013.

[159] S. N. Qu, X. Y. Wang, Q. P. Lu, X. Y. Liu, and L. J. Wang, "A biocompatible fluorescent ink based on water-soluble luminescent carbon nanodots," *Angewandte Chemie—International Edition*, vol. 51, no. 49, pp. 12215–12218, 2012.

[160] A. B. Bourlinos, R. Zbořil, J. Petr, A. Bakandritsos, M. Krysmann, and E. P. Giannelis, "Luminescent surface quaternized carbon dots," *Chemistry of Materials*, vol. 24, no. 1, pp. 6–8, 2012.

[161] A. B. Bourlinos, M. A. Karakassides, A. Kouloumpis et al., "Synthesis, characterization and non-linear optical response of organophilic carbon dots," *Carbon*, vol. 61, pp. 640–643, 2013.

[162] G. E. Lecroy, S. K. Sonkar, F. Yang et al., "Toward structurally defined carbon dots as ultracompact fluorescent probes," *ACS Nano*, vol. 8, no. 5, pp. 4522–4529, 2014.

[163] J.-Y. Yin, H.-J. Liu, S. Jiang, Y. Chen, and Y. Yao, "Hyperbranched polymer functionalized carbon dots with multi-stimuli- responsive property," *ACS Macro Letters*, vol. 2, no. 11, pp. 1033–1037, 2013.

[164] A. Prasannan and T. Imae, "One-pot synthesis of fluorescent carbon dots from orange waste peels," *Industrial & Engineering Chemistry Research*, vol. 52, no. 44, pp. 15673–15678, 2013.

[165] S. Nandi, R. Malishev, K. Parambath Kootery, Y. Mirsky, S. Kolusheva, and R. Jelinek, "Membrane analysis with amphiphilic carbon dots," *Chemical Communications*, vol. 50, no. 71, pp. 10299–10302, 2014.

[166] J. K. Navin, M. E. Grass, G. A. Somorjai, and A. L. Marsh, "Characterization of colloidal platinum nanoparticles by MALDI-TOF mass spectrometry," *Analytical Chemistry*, vol. 81, no. 15, pp. 6295–6299, 2009.

[167] I. P. Matthews, C. J. Gregory, G. Aljayyoussi et al., "Maximal extent of translocation of single-walled carbon nanotubes from lung airways of the rat," *Environmental Toxicology and Pharmacology*, vol. 35, no. 3, pp. 461–464, 2013.

[168] A. Scheffer, C. Engelhard, M. Sperling, and W. Buscher, "ICP-MS as a new tool for the determination of gold nanoparticles in bioanalytical applications," *Analytical and Bioanalytical Chemistry*, vol. 390, no. 1, pp. 249–252, 2008.

[169] C. Ispas, D. Andreescu, A. Patel, D. V. Goia, S. Andreescu, and K. N. Wallace, "Toxicity and developmental defects of different sizes and shape nickel nanoparticles in zebrafish," *Environmental Science and Technology*, vol. 43, no. 16, pp. 6349–6356, 2009.

[170] S. Xie, M. C. Paau, Y. Zhang, S. Shuang, W. Chan, and M. M. F. Choi, "High-performance liquid chromatographic analysis of as-synthesised N,N′-dimethylformamide-stabilised gold nanoclusters product," *Nanoscale*, vol. 4, no. 17, pp. 5325–5332, 2012.

[171] Y. Zhang, S. Shuang, C. Dong, C. K. Lo, M. C. Paau, and M. M. F. Choi, "Application of HPLC and MALDI-TOF MS for studying as-synthesized ligand-protected gold nanoclusters products," *Analytical Chemistry*, vol. 81, no. 4, pp. 1676–1685, 2009.

[172] Y. Zhang, Q. Hu, M. C. Paau et al., "Probing histidine-stabilized gold nanoclusters product by high-performance liquid chromatography and mass spectrometry," *Journal of Physical Chemistry C*, vol. 117, no. 36, pp. 18697–18708, 2013.

[173] Q. Hu, X. Meng, M. M. F. Choi, X. Gong, and W. Chan, "Elucidating the structure of carbon nanoparticles by ultra-performance liquid chromatography coupled with electrospray ionisation quadrupole time-of-flight tandem mass spectrometry," *Analytica Chimica Acta*, vol. 911, pp. 100–107, 2016.

[174] V. N. Mehta, S. Jha, R. K. Singhal, and S. K. Kailasa, "Preparation of multicolor emitting carbon dots for HeLa cell imaging," *New Journal of Chemistry*, vol. 38, no. 12, pp. 6152–6160, 2014.

[175] D. Li, X. Hu, Q. Li et al., "Self-assembled long-chain organic ion grafted carbon dot ionic nanohybrids with liquid-like behavior and dual luminescence," *New Journal of Chemistry*, vol. 37, no. 12, pp. 3857–3860, 2013.

[176] F. d'Orlyé, A. Varenne, and P. Gareil, "Size-based characterization of nanometric cationic maghemite particles using capillary zone electrophoresis," *Electrophoresis*, vol. 29, no. 18, pp. 3768–3778, 2008.

[177] U. Pyell, "CE characterization of semiconductor nanocrystals encapsulated with amorphous silicium dioxide," *Electrophoresis*, vol. 29, no. 3, pp. 576–589, 2008.

[178] N. G. Vanifatova, B. Y. Spivakov, J. Mattusch, U. Franck, and R. Wennrich, "Investigation of iron oxide nanoparticles by capillary zone electrophoresis," *Talanta*, vol. 66, no. 3, pp. 605–610, 2005.

[179] F.-K. Liu, F.-H. Ko, P.-W. Huang, C.-H. Wu, and T.-C. Chu, "Studying the size/shape separation and optical properties of silver nanoparticles by capillary electrophoresis," *Journal of Chromatography A*, vol. 1062, no. 1, pp. 139–145, 2005.

[180] F.-K. Liu, M.-H. Tsai, Y.-C. Hsu, and T.-C. Chu, "Analytical separation of Au/Ag core/shell nanoparticles by capillary electrophoresis," *Journal of Chromatography A*, vol. 1133, no. 1-2, pp. 340–346, 2006.

[181] D. A. Eckhoff, J. N. Stuart, J. D. B. Sutin, J. V. Sweedler, and E. Gratton, "Capillary electrophoresis of ultrasmall carboxylate functionalized silicon nanoparticles," *Journal of Chemical Physics*, vol. 125, no. 8, Article ID 081103, 2006.

[182] A. I. López-Lorente, B. M. Simonet, and M. Valcárcel, "Electrophoretic methods for the analysis of nanoparticles," *Trends in Analytical Chemistry*, vol. 30, no. 1, pp. 58–71, 2011.

[183] K. L. Chung, C. P. Man, D. Xiao, and M. M. F. Choi, "Capillary electrophoresis, mass spectrometry, and UV-visible absorption studies on electrolyte-induced fractionation of gold nanoclusters," *Analytical Chemistry*, vol. 80, no. 7, pp. 2439–2446, 2008.

[184] C. K. Lo, M. C. Paau, D. Xiao, and M. M. F. Choi, "Application of capillary zone electrophoresis for separation of water-soluble gold monolayer-protected clusters," *Electrophoresis*, vol. 29, no. 11, pp. 2330–2339, 2008.

[185] H.-P. Jen, Y.-C. Tsai, H.-L. Su, and Y.-Z. Hsieh, "On-line preconcentration and determination of ketamine and norketamine by micellar electrokinetic chromatography: Complementary method to gas chromatography/mass spectrometry," *Journal of Chromatography A*, vol. 1111, no. 2, pp. 159–165, 2006.

[186] A. M. Gole, C. Sathivel, A. Lachke, and M. Sastry, "Size separation of colloidal nanoparticles using a miniscale isoelectric focusing technique," *Journal of Chromatography A*, vol. 848, no. 1-2, pp. 485–490, 1999.

[187] X. Gong, M. Chin Paau, Q. Hu, S. Shuang, C. Dong, and M. M. F. Choi, "UHPLC combined with mass spectrometric study of as-synthesized carbon dots samples," *Talanta*, vol. 146, pp. 340–350, 2016.

[188] L. Bai, X. Ma, J. Liu, X. Sun, D. Zhao, and D. G. Evans, "Rapid separation and purification of nanoparticles in organic density gradients," *Journal of the American Chemical Society*, vol. 132, no. 7, pp. 2333–2337, 2010.

[189] J.-F. Liu, S.-J. Yu, Y.-G. Yin, and J.-B. Chao, "Methods for separation, identification, characterization and quantification of silver nanoparticles," *TrAC - Trends in Analytical Chemistry*, vol. 33, pp. 95–106, 2012.